

UNIVERSITY OF THE WITWATERSRAND

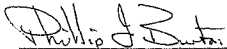
A SIMULATION OF THE  
FOSKUR FLOTATION PLANT

P.F. BURTON

DECLARATION

I hereby certify that this research, unless where specifically acknowledged, is the result of my own investigation which has not already been accepted in substance for any degree and is not being concurrently submitted in candidature for any other degree.

All experimentation was carried out at the research department of the Phosphate Development Corporation. The computations, using the simulator, were undertaken at the University of the Witwatersrand.



PHILLIP FREDERICK BURTON

A SIMULATION OF THE  
FOSKOR FLOTATION PLANT

PHILLIP FREDERICK BURTON

A Dissertation submitted to the Faculty of Engineering,  
*University of the Witwatersrand, Johannesburg* for the  
Degree of Master of Science

Johannesburg 1978

ACKNOWLEDGEMENTS.

I wish to express my thanks to the Phosphate Development Corporation for the use of their research facilities, and co-operation I received when carrying out work in the plant.

I would also like to thank:-

Professor R.P. King, my supervisor, for his guidance and advice throughout the project

Mrs. D. Harnden, for her patience and help with the setting out and typing of this thesis.

SYNOPSIS

A simulator to predict the performance of the Foskor plant was investigated. The kinetic parameters required for the simulator were obtained from the batch flotation of a standard ore, conditioned old plant feed, unconditioned new plant feed, and unconditioned P.M.C. tailings, also from continuous experiments carried out on the rougher bank of the old and new plants.

The kinetic parameters obtained from the batch flotation of unconditioned feed gave comparable results, but with a wide 95% confidence band, while the conditioned old plant feed gave equivalent results but a narrow 95% confidence band. Those parameters obtained from the continuous experiments gave very wide 95% confidence bands and the average results differed from the batch experiments by a factor of 2 and 0,5 for the old plant and new plant respectively.

The description of both the old and new plants was best given by the kinetic parameters obtained from the batch flotation of conditioned old-plant feed.

## CONTENTS

	<u>PAGE</u>
1 Introduction	
1.1 Statement of problem	1
1.2 Why problem exists	1
1.3 Experimental programme	2
1.4 System to be studied	2
2 Mineralogical study of Foskorite	
2.1 Phalaborwa igneous complex	6
2.1.1 Central carbonatite body	6
2.1.2 Surrounding body of Foskorite ore	6
2.1.3 Massive Pyroxenite ore body	6
2.2 Liberation of minerals in Foskorite ore	8
2.2.1 Microscopic examination of foskorite	8
2.2.2 Determination of the liberation of apatite and calcite	8
2.2.2.1 Magnetic separation	9
2.2.2.2 Heavy liquid separation	11
2.2.3 Discussion of Results	13
2.3 Classification of Foskorite	17
3 Estimation of model parameters	
3.1 The Flotation Model	18
3.2 Particle size determination	19
3.2.1. Assay analysis	21

	<u>PAGE</u>
3.3 Effect of particle size on the rate of flotation	21
3.4 Aeration Rate	26
3.5 Froth transmission coefficient	26A
3.6 Specific rate constant	26B
3.6.1 Batch Tests	
3.6.1.1 Standard Ore	26B
3.6.1.2 Conditioned Rougher Feed	41
3.6.1.3 Unconditioned New Plant Feed	45
3.6.1.4 P.M.C. unconditioned tailings feed	60
3.6.2 Continuous Test	
3.6.2.1 Old Plant	73
3.6.2.2 New Plant	77
3.7 Discussion on the specific rate constant values	
3.7.1 Standard ore	81
3.7.2 Conditioned rougher feed	87
3.7.3 Batch tests on new plant feed	88
3.7.4 Batch tests on P.M.C. tailings feed	89
3.7.5 Continuous runs, old and new plant	90
3.7.6 Mean kinetic parameters	91
4 Simulation of Foskor Plant	
4.1 Simulation of old plant rougher bank	95
4.1.1 Simulation using gamma calculated from water ratio	
4.1.1.1 Percent apatite in concentrate streams	110
4.1.1.2 Mass flow rate in concentrate streams	110

v

	<u>PAGE</u>
4.1.2 Simulation using gamma equal to unity	
4.1.2.1 Percent apatite in concentrate streams	111
4.1.2.2 Mass flow rate in concentrate streams	111
4.2 Daily simulations of old plant	112
4.3 Simulation of new plant	120
5 Discussion and Conclusions	
5.1 Kinetic parameters	134
5.2 Froth transmission coefficient	135
5.3 General	135

CHAPTER 1.

INTRODUCTION

1.1 Statement of the Problem

Over the past decade much work has been carried out into developing models of flotation plants. The approach to that work has been to derive kinetic equations to represent what is actually taking place in the flotation process.

It has been shown in the literature (1,2) that kinetic models can adequately describe the behaviour of single cells (batch or continuous), pilot plants and the cleaner banks of a continuous operating plant.

The scope of this dissertation is to investigate how well the model developed by the National Institute for Metallurgy describes an industrial operating plant with all its attendant variables.

In brief the problem may be stated as follows. How, from an industrial plant, can the necessary parameters required to set up the model best be measured. That is to say, can the required model parameters be determined by batch tests carried out in the laboratory or must they be obtained from the continuous operating plant. Also do the estimated parameters from the laboratory agree with those from the plant, if not why, and then which of the parameter estimates best predict the plant performance when the kinetic model is used to simulate plant performance.

1.2 Why the problem exists

The proposed use of the simulator is not to replace either the laboratory or pilot plant test work, but to act as a guide to the

direction such work should take, and so alleviate unnecessary experimentation. Also plant configurations that could not be tried out on an operating plant, because of extensive piping alteration and loss of production could be carried out. Those configurations that the simulator predicts should increase production, can then be tested on a pilot plant scale. Thus the model can short circuit the normal lengthy experiments required to test out various plant configurations.

### 1.3 Experimental programme

As will be set out later in the dissertation, the main parameters for the model that can not be directly measured are the kinetic flotation parameters. These have to be determined by either batch flotation in the laboratory or from measurements carried out on the continuous running plant. At Foskor it is already known that the reagent dosage used in the laboratory are different from those used in the plant. It is thought that these differences can be attributed to the circulating masses of solids and water, both of which carry with them flotation reagents. Thus a measure of the difference, if any, between the kinetic parameters measured in the laboratory and plant is of fundamental interest.

The kinetic flotation parameters of foskorite ore were measured in the following series of experiments. The first series of experiments consisted of laboratory batch flotation tests carried out on a representative ore sample (standard ore), old plant conditioned rougher feed, new plant unconditioned feed and unconditioned P.M.C. tailings feed. The second series consisted of measuring the parameters from the continuously operating plant. These experiments were carried out on 50 cubic feet rougher cells (old plant) and 300 cubic feet rougher cells (new plant). Figs 18 and 32 show the layout of the plants.

Component	Foskorite Feed	Pyroxenite Feed	Foskorite Concentrate	Pyroxenite Concentrate
P <sub>2</sub> O <sub>5</sub>	8.0	7.5	37.5	37.5
CaO	23.6	24.9	53.7	53.0
CO <sub>2</sub>	10.9	0.8	3.6	2.9
Fe <sub>2</sub> O <sub>4</sub>	28.5	2.3	0.35	0.27
MgO	12.7	14.5	0.76	1.06
TiO <sub>2</sub>	2.1	0.5	.04	Trace
ZrO <sub>2</sub>	0.6	0.05	Trace	Trace
Rare Earths	0.1	0.2	0.4	0.7
F	0.73	0.74	2.2	2.2
SiO <sub>2</sub>	10.0	35.6	-	-
Acid Insoluble	-	-	0.09	2.0
MnO	0.54	0.05	0.02	0.01
K <sub>2</sub> O	0.78	2.10	0.01	0.05
Na <sub>2</sub> O	0.46	0.67	0.07	0.04
Cu	0.23	0.004	-	-
Ni	0.02	0.01	-	-
S	0.1	Trace	-	-
Al <sub>2</sub> O <sub>3</sub>	2.5	6.4	0.05	0.15
Cl <sub>2</sub>	Trace	Trace	Trace	Trace

Table 1 Analysis of Phosphate feed and concentrate

RELATIVE PROPORTION OF CONSTITUENTS	MINERALS	COMPOSITION
Major	Calcite Magnetite	CaCO <sub>3</sub> FeO . Fe <sub>2</sub> O <sub>3</sub>
Subordinate	Apatite Phlogopite Olivine	Ca <sub>4</sub> (CaF) (PO <sub>4</sub> ) <sub>3</sub> H <sub>2</sub> Mg <sub>3</sub> Al (SiO <sub>4</sub> ) <sub>3</sub> (MgFe) <sub>2</sub> SiO <sub>4</sub>
Minor to Trace	Diopside Bornite Chalcopyrite Monozite	CaO . MgO . 2SiO <sub>2</sub> Cu <sub>5</sub> FeS <sub>4</sub> CuFeS <sub>2</sub> (CeLaDy) PO <sub>4</sub> ThSiO <sub>4</sub>

Table 1a Analysis of Feskorite Ore

1.4 System to be studied

The kinetic parameters that have been estimated are those of an ore type known as "foskorite". This ore is obtained from the Phalaborwa complex in the Eastern Transvaal. An analyses of this ore is shown in table 1 and 1(a). The initial work on the froth flotation of foskorite was done by Preller (3). The reagents used to float this ore are:-

- a) Unitol D.S.R. - tall oil fatty acid, which acts as a frother/collector.
- b) Berol E.M.U. - poly-glycol ether, which is a dispersant and froth modifier.
- c) Sodium silicate - a dispersant and calcite depressant.
- d) Sodium hydroxide - pH regulator.

Due to the complex nature of the ore body, there is no guaranteed reagent combination that will float the ore. The method used at Foskor, in the research department, is to start with a fixed ratio of reagents, then to raise and lower each one in turn until a "good" float is obtained. Although this method is subjective it is reliable. A point to be argued against laboratory batch test work, is that the floats are so good as to be unrepresentative of the plant, where the control over the float is more difficult.

CHAPTER II.

MINERALOGICAL STUDY OF FOSKORITE

2.1 Phalaborwa igneous complex (4)

This igneous complex is a cylindrical intrusion in the granites of the archaic era consisting of the following discrete ore bodies as illustrated in Figure 1.

2.1.1 Central Carbonatite body

The ore has a low phosphate content (1,25 - 2,5% P), but an economically mineable copper content of between 0,5 - 0,8% Cu. Associated with these minerals are baddeleyite (natural  $ZrO_2$ ), uranium and magnetite with a low titanium content ( $< 1\% TiO_2$ ).

2.1.2 Surrounding body of Foskorite ore

It differs in two important aspects from the carbonatite. The phosphate content is higher (3,5 - 4,8% P) and the titanium content of the magnetite is higher (3 - 5%  $TiO_2$ ). The main diluent minerals in the above two mentioned bodies are olivine-serpentine, carbonatite and phlogopite.

2.1.3 Massive Pyroxenite ore body

This body is 6 km long and 3 km wide with an average phosphate content of 2,5 - 3,5% P. The main diluent minerals are diopside and phlogopitic-vermiculite. Apatite, the phosphate bearing ore, is the only mineral of economic importance.

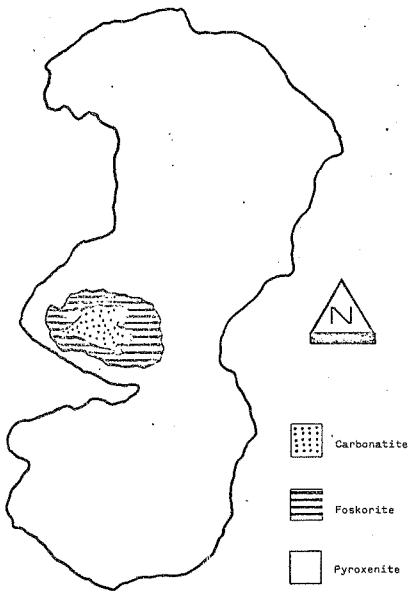


Figure 1 Phalaborwa Igneous Complex

## 2.2 Liberation of minerals in Foskorite ore

A mineralogical study of Foskorite was undertaken to determine the liberation of mineral species. This was achieved by using the following techniques; microscopic examination, magnetic separation, and heavy liquids.

### 2.2.1 Microscopic examination of Foskorite

Various size fractions of foskorite ore were examined microscopically. All fractions examined (-417/+295 microns to -74/+43 microns) showed complete liberation of apatite from serpentine and phlogopite; and greater than 95% liberation of magnetite. These magnetite inclusions in apatite were in the form of finely disseminated particles. The liberation of apatite from calcite could not be determined microscopically due to the similarity in colour and texture of the minerals.

### 2.2.2 Determination of the liberation of apatite and calcite

To determine the liberation of apatite and calcite, these minerals had to be separated from the other minerals that make up foskorite. Apatite has a negative magnetic susceptibility and calcite a low but positive magnetic susceptibility, all the other minerals have a high positive susceptibility. Because of these differences in magnetic susceptibility magnetic separation using the Frantz isodynamic separator, was used as the technique for obtaining samples of apatite and calcite.

2.2.2.1 Magnetic separation

The Frantz isodynamic separator is used to separate out minerals having low but different magnetic susceptibilities. It consists of a vibrating chute mounted centrally between the pole pieces of an electro-magnet. This unit may be inclined in any direction by a universal mounting, and the electro-magnetic current is continuously adjustable from 0 to 1,5 amperes.

A sample of Standard Ore Foskorite was dry sieved through Tyler screens and the +147/-295 micron size fraction retained Magnetite was then removed using a hand magnetic separator from this size fraction. The non-magnetic fraction was weighed. The Frantz isodynamic separator was set with a longitudinal angle of +25° and a transverse slope of +20°, with a current setting of zero. The non-magnetics were then loaded into the hopper of the separator, and the chute vibrator activated. The resulting magnetic and non-magnetic fractions were weighed. The current was then adjusted to 0,1 amp and the non-magnetics placed in the hopper, the chute vibrator was again activated. This procedure was repeated for current values of 0,3 0,5 0,7 and 1,0 amperes, the magnetic fractions being retained. Table 2 shows the results from the separation.

Field current, amps	0,0	0,1	0,3	0,5	0,7	1,0
Longitudinal angle	25	25	25	25	25	25
Transverse angle	20	20	20	20	20	20
Mass of magnetic fraction	0,032	33,4	46,9	16,1	12,1	12,5
Fractional distribution of magnetics,	0	0,181	0,254	0,087	0,065	0,068
Cumulative distribution	0	0,181	0,435	0,522	0,587	0,655

Table 2 Dry Magnetic Separation using the Frantz Isodynamic Separator

Total Mass : 186,3g

Material tested : Fostest Sample No. 2 -205  $\mu$ m +147  $\mu$ m

The transverse angle of the separator was then adjusted to  $+15^\circ$  and the non-magnetic fraction from the 1,0 ampere separation loaded into the hopper, the chute vibrator was then activated. The current being kept at 1,0 ampere. The resulting magnetic and non-magnetic fractions were weighed. Then the transverse angle was adjusted to  $+10^\circ$  and the non-magnetics loaded. This procedure was repeated for transverse angles 6, 4, 2 and  $0^\circ$ , the magnetic fractions being retained. Table 3 shows the results from the separation.

Visual examination of the magnetic fractions from the 0, 2, 4 and  $6^\circ$  transverse angle separations and also the final non-magnetic fraction showed that the majority of the particles were either colourless or opaque white. To determine the amount of liberation between apatite and calcite heavy liquid separation was used.

#### 2.2.2.2 Heavy liquid separation

The specific gravities of apatite and calcite are 3,2 and 2,71 (5), thus are amenable to heavy liquid separation. The heavy liquid mediums used were tetrabromoethane (sg 2,94) and methylene iodide (sg 3,3). To obtain a range of densities from 2,0 to 2,94 mixtures of acetone (AR) and tetrabromoethane were prepared : for densities between 2,94 and 3,33 mixtures of tetrabromoethane .



Field current, amps	1,0	1,0	1,0	1,0	1,0	1,0	1,0	1,0	1,0
Longitudinal angle	25	25	25	20	20	20	20	20	20
Transverse angle	20	15	10	6	4	2	0	0	0
Mass of magnetic fraction	12,5	8,26	10,51	10,80	9,08	10,84	11,14		
Fractional distribution of magnetics	0,163	0,108	0,137	0,142	0,118	0,141	0,149		
Cumulative distribution of magnetics	0,163	0,272	0,408	0,550	0,668	0,809	0,958		

Table 3 Dry Magnetic Separation using the Frantz Isodynamic Separator  
Total Mass : 63,9g  
Material Tested : Footeest Sample No. 2 - Non-magnetic fraction from Table 2

and methylene iodide were used.

The samples that were separated by heavy liquids were those magnetic fractions with a transverse angle of 0, 2, 4 and 6° with an electromagnetic current of 1.0 amperes. Also examined was the final non-magnetic fraction.

A weighed sample (ca 1.5 g) was placed in a heavy liquid column containing tetrabromoethane. After a suitable time (30 - 60 minutes) both the sink and float fractions were removed, washed with acetone, dried and weighed. The sink fraction (sg > 2.94) was transferred to a heavy liquid column containing a mixture of tetrabromoethane and methylene iodide, and sink/float fractions were obtained. This procedure was repeated on the successive sink fractions at four different specific gravities. The same procedure was adopted for the initial float fraction (sg < 2.94), but this time using tetrabromoethane and acetone (AR) as the heavy liquid medium. The method of determining the density of the heavy liquid is given in appendix 1. Figures 2 - 6 show the specific gravity vs cumulative float fraction for the samples examined.

### 2.2.3 Discussion of results

The two significant features of the Figures 2 - 6 are the plateau and the vertical lines at sg 2.72 and 3.2.

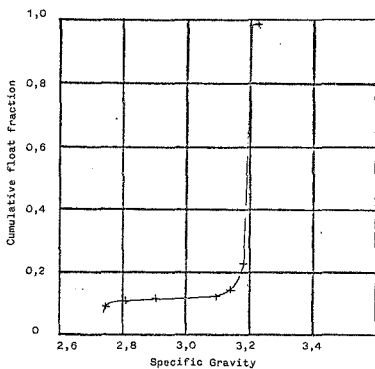


Figure 2 Cumulative distribution function for non-magnetic fraction of ore

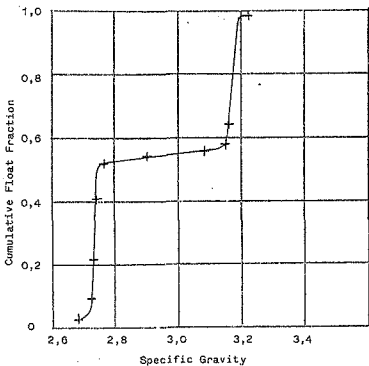


Figure 3 Cumulative float fraction vs. specific gravity of magnetic material obtained at transverse angle 0

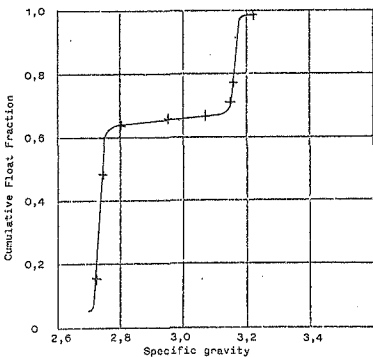


Figure 4 Cumulative float fraction vs. specific gravity of magnetic material obtained at transverse angle +2

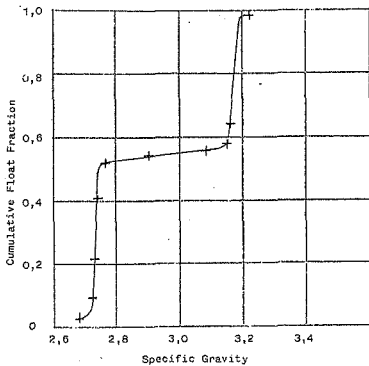


Figure 3 Cumulative float fraction vs. specific gravity of magnetic material obtained at transverse angle 0

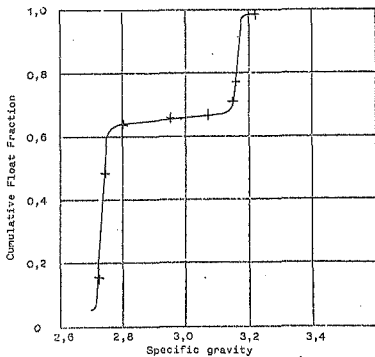


Figure 4 Cumulative float fraction vs. specific gravity of magnetic material obtained at transverse angle +2

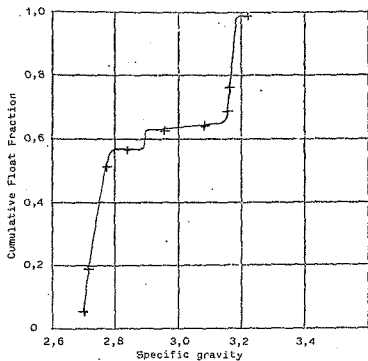


Figure 5 Cumulative float fraction vs. specific gravity of magnetic material obtained at transverse angle +4

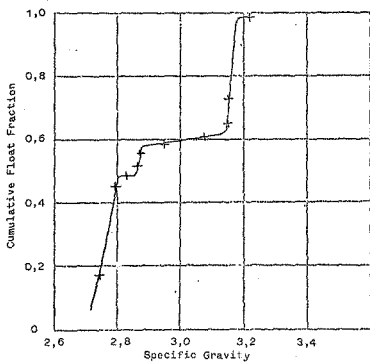


Figure 6 Cumulative float fraction vs. specific gravity of magnetic material obtained at transverse angle +6

The steepness of the steps in the distribution function at sg 2,72 and 3,2 and the horizontal plateau between shows that there is virtually complete liberation between apatite and calcite. The slightly larger magnetic susceptibility of the calcite is evident from the larger calcite fractions in the magnetic fractions at the larger angles in figures 3 and 4.

Figure 2, which is the final non-magnetic fraction, shows that approximately 90% of this fraction is pure apatite and 10% calcite. Figures 3 and 4 show the same complete liberation of apatite and calcite but with a greater amount of calcite occurring at the higher angle. Figures 5 and 6 also show that the apatite is completely liberated but with a third mineral occurring at these higher angles. This third mineral, phlogopite, has a sg. of 2,8 and is completely liberated from both apatite and calcite (Figure 6) as indicated by the plateau and vertical line.

### 2.3 Classification of Foskorite

From the microscopic examination and heavy liquid separation carried out on foskorite the ore can be classified into two species so far as flotation is concerned : apatite, the valuable mineral and gangue, all other minerals. These mineral classes will be referred to as G classes. Thus mineral class G<sub>1</sub> will refer to apatite and mineral class G<sub>2</sub> to gangue. No unliberated mineral classes need be examined or allowed for in the model.

CHAPTER 3.

ESTIMATION OF MODEL PARAMETERS

3.1 The Flotation model

The investigation undertaken was not to develop a new model, but to use the existing one developed by the National Institute for Metallurgy, and test its adequacy to predict the performance of the Foskor plant. The modification of the model or the simulator was outside the scope of this investigation.

The model chosen is one that recognizes the similarity between the flotation process and a first order chemical reaction. That is to say the fundamental basis for the modelling of a flotation cell is that the rate at which material leaves the pulp is a strong function of the amount of that particular kind of material present in the pulp. It also takes into account that the system is not homogeneous, in that particles of ore differ one from another and must be treated differently.

The model classifies particles into discrete classes of size, mineral content, and flotation rate constant. It assumes that there is no interaction between classes when the average is taken over the entire heterogeneous population for the modelling of the rate in the cell containing many different particle types.(6)

The difficulty with a distributed rate constant model is that there are a great number of variables generated, both state variables such as particle size, mineral type, and model parameters of which there is correspondingly a large number. This problem is overcome by considering only a few groups with differing properties. The assumption is then that the solid particles entering a system can be classified according to their flotation behaviour, and a number of discrete classes considered based on particle size (D-class), degree of liberation (G-class), and flotation rate constant (K-class). The first two of these can be measured directly, but the third must be obtained from

observation of the ore in a flotation cell. Bubble loading is accounted for according to the model of Pogorely (7). The water balance in the model is determined on the assumption that the percent solids in the concentrate stream is known as primary data. The holding times are calculated internally. There is no restriction on plant configuration.

The model is based upon the equation rate of flotation =  $\bar{X} k \phi (G,D) A S C$  where  $\bar{X}$  is the fraction of floated material that passes into the concentrate stream,  $k$  is the specific rate constant,  $\phi (G,D)$  is the fractional efficiency for flotation of particles of size  $D$ ,  $A$  is the bubble surface area per unit volume of the cell,  $S$  is the fraction of the bubble area that is not covered by adhering particles, and  $C$  is the concentration of particles of a particular class in the cell.

### 3.2. Particle size determination (D-class)

The flotation feed samples were classified into nine fractions using Tyler standard screens. Figure 7 shows the particle size distribution vs. percent mass retained. The shallower the slope the more even the distribution of particles. The five curves shown are for P.M.C. tailings, standard ore, old plant rougher feed, old plant feed and new plant feed.

The standard ore sample was rod milled in the laboratory to give a profile as near ideal as possible. P.M.C. tailings comes from the final copper tailings stream after a re-grind has been carried out on the primary copper tailings, and the liberated copper removed. It is due to the regrinding step that

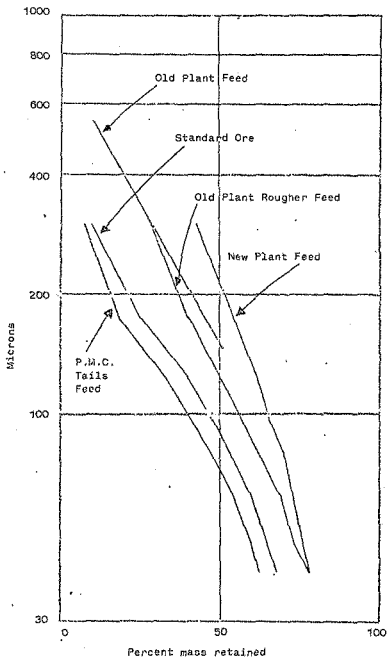


Figure 7 Particle size distribution vs. percent mass retained

the curve is so shallow. The old plant rougher feed contains plant feed plus the recirculating loss from the scavenger concentrate and cleaner tails, this accounts for its steeper slope compared to the old plant feed. (8) The new plant feed shows a very steep profile indicating the poor performance of the mills at higher tonnages.

### 3.2.1. Assay Analysis

The phosphate analysis was carried out by the analytical department at Foskor. The analysis is a photometric method using molybdovanadate reagent. Replicate samples were sent for analysis to check the variance of the analytical method. The results of these replicate samples showed that over a range of  $P_2O_5$  values (2,4 %  $P_2O_5$  to 29,7 %  $P_2O_5$ ) the average error was  $\pm 0,6$  %. Samples having a  $P_2O_5$  content between 2,4 %  $P_2O_5$  and 2,9 %  $P_2O_5$  had an error of  $\pm 1,9$  %. Appendix 2 gives the comparison of results for the replicate analysis.

### 3.4 Effect of particle size on the rate of flotation

The effect of particle size on the rate of flotation has been taken into account by Colborn's  $\Theta$  (D) factor.(9). This assumes that all particles having the same mineral content are affected in the same relative way by particle size, independent of the rate constant assigned to the particular mineral class. Colborn was able to correlate his observations with  $\Theta$  (D) =  $2,33 (\epsilon / D^2)^{1/4} \exp(-\epsilon / D^2) (1 - (D/\Delta))^{1,5}$  where  $\Delta$  is the largest particle floated, D is the particle size and  $\epsilon$  is the turbulence intensity which is approximately equal to  $0,5 D^2 \max$  where  $D \max$  is the particle size.

that has the largest rate of flotation. Each mineral class has a specific pair of values for  $\bar{E}$  and  $\Delta$ . Thus two  $\theta(D)$  curves were required for foskorite, one for apatite the other for the gangue minerals.

Colborn's function was calculated for fresh feed and also for the old plant rougher feed.

#### 3.4.1. Colborn's function for fresh feed

An assay sieve analysis was carried out on the feed and the first concentrate sample of an incremental float. For each size fraction the recovery is calculated and a plot of  $\ln(1 - R(G,D))$  against particle size gives the functional form of  $\theta(G,D)$  (17,18).  $R(G,D)$  is the fractional recovery of size  $D$  and composition  $G$ . This was carried out for both mineral (apatite) and gangue. An average assay sieve analysis for both feed and first concentrate sample of the standard ore series is shown in Table 4. Figures 8 and 9 show the  $\theta(G,D)$  curves for apatite and gangue respectively. Using these experimental curves the value of  $D_{max}$  and  $\Delta$  were determined and the  $\theta(G,D)$  curve was then calculated and plotted. Due to experimental errors the value of  $D_{max}$  could not always be precisely determined to a trial and error technique was used until a best fit was obtained.

#### 3.4.2. Colborn's function for a continuous rougher bank

To calculate the recovery on the continuous operating rougher bank, an assay sieve analysis was carried out on

Assay sieve analysis		Average micron size									
		300	175	124	96	81	63	48	40	30	
Feed	Mass percent	10,20	15,12	15,16	7,46	5,26	6,76	5,02	3,30	31,80	
	Percent Apatite	15,3	32,7	39,7	41,5	42,0	42,7	42,9	43,0	34,8	
First Concen- trate	Mass percent	4,37	13,34	16,91	9,55	7,88	8,63	5,98	4,03	29,33	
	Percent Apatite	72,3	83,2	80,1	77,1	72,8	69,5	65,9	65,0	51,1	

Colborn's function		Average micron size									
		300	175	124	96	81	63	48	40	30	
Apatite	Experimental	0,57	0,85	0,74	0,83	0,98	0,70	0,04	0,46	0,32	
	Calculated	0,37	0,64	0,84	0,95	0,98	0,91	0,73	0,60	0,43	
Gangue	Experimental	0,11	0,32	0,51	0,66	0,76	0,83	0,81	0,83	0,71	
	Calculated	0,02	0,26	0,45	0,61	0,71	0,86	0,94	0,92	0,80	

Table 4 Average assay sieve analysis for standard ore feed and first concentrate with the estimated and predicted values of Colborn's function

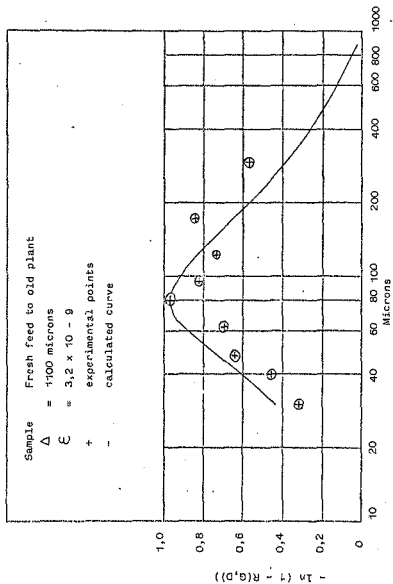


Figure 8 Specific rate constant for apatite as a function of particle size

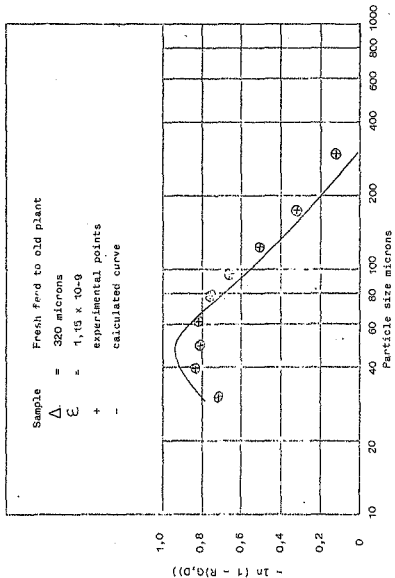


Figure 9 Specific flotation rate constant for gangue as a function of particle size

the rougher feed, combined concentrate and rougher tails. A plot of  $R(G,D)/(1 - R(G,D))$  against particle size gave the experimental  $\theta(G,D)$  curve. Figures 9a and 10 show the experimental and calculated  $\theta(G,D)$  curves for apatite and gangue respectively. Table 5 gives the average assay sieve analysis for the rougher feed, and combined concentrate.

In the following work the  $\theta(G,D)$  curve obtained from the fresh feed was used for calculations involving the batch flotation of standard ore, while the  $\theta(G,D)$  curve obtained from the old plant rougher circuit was used for all other parameter estimations. Furthermore the function obtained from the old plant rougher was also used in the simulations of both the old and new plants, and also the daily simulations.

From figure 3 it can be noted that the recovery in the laboratory batch cell is significantly higher in the larger particle sizes. This probably reflects better flotation conditions obtainable in the laboratory. Consequently the data collected from the plant was considered to be more representative. It should be noted that the old plant rougher feed contained middlings returned from the scavenger concentrate and cleaner tails, while the fresh feed contained no circulating material.

#### 3.4 Aeration Rates

The effect of aeration rate can be modelled in a very simple way by postulating that the rate of flotation is proportional to the available surface area of bubbles per unit volume of pulp.

The relationship can be written thus:-

$$A = \frac{\sigma \gamma G}{V}$$

where A = bubble surface area per unit volume of pulp

$\sigma$  = bubble surface area per unit volume of bubble

$\gamma$  = average bubble residence time

V = cell volume

G = aeration rate

The above equation is the main scale up relation for the flotation cell.  $\gamma$  varies with the size of the cell, and  $\sigma$ , which is determined by the shape and size of bubble, varies with the size of the cell and the dispersion and agitation mechanism.

Throughout this work the bubble size was assumed to have the same value (2mm) in each of the flotation cell types. This assumption undoubtedly accounts for some of the variation in rate constant found from cell to cell during the investigation. However, visual observation indicated that large variations in bubble size could not be expected and the measurement of mean bubble size in each cell (a difficult and time consuming procedure) was not considered justified in this study.

### 3.5 Froth transmission coefficient

The direct measurement of the froth transmission coefficient is as yet not possible. This coefficient is defined as the ratio of solids flow rate across the froth lip to that across the pulp froth interface. It has been suggested (10) that an estimate of the froth transmission coefficient can be obtained from  $\gamma_i = q_i / g_i$  where  $\gamma_i$  is the froth transmission coefficient for the  $i^{\text{th}}$  stage and  $g_i$  is the water flow rate in the  $i^{\text{th}}$  stage.

In the plant circuits, for flotation parameter estimates, gamma was calculated as the ratio of measured water rate in the concentrate to the maximum water production rate in the concentrate streams, from any cell in the rougher. This is consistent with the method used for the estimation of flotation parameters from the batch tests.

Using the above method, the froth transmission coefficient was estimated for the scavenger, cleaner and recleaner circuits, (no iterative calculations were necessary). It was noted that the cells in the cleaner and recleaner bank produced froths significantly different in character from these in the rougher bank. This difference was characterized by the cleaner and recleaner froths being of a more brittle and tighter nature than the rougher or scavenger. Due to the froth being brittle there was a high froth breakage rate but less of the solids appeared to return from the froth phase to the pulp as compared to the water. Thus it was felt reasonable to assume that the froth transmission coefficient for the cleaner and recleaner was between the water ratio and unity.

For the simulations of the new plant the froth transmission coefficient was assumed to be constant throughout the plant and adjusted to get a good fit between predicted and experimental data.

### 3.6 Estimation of specific rate constant

#### 3.6.1 Batch flotation

##### 3.6.1.1. Standard ore

A representative batch of foskorite ore (150 kg) was collected over a period of eight hours from six ribbon feeders to the rod mills at the Foskor plant. The maximum lump size in this sample was 2 cm. The ore

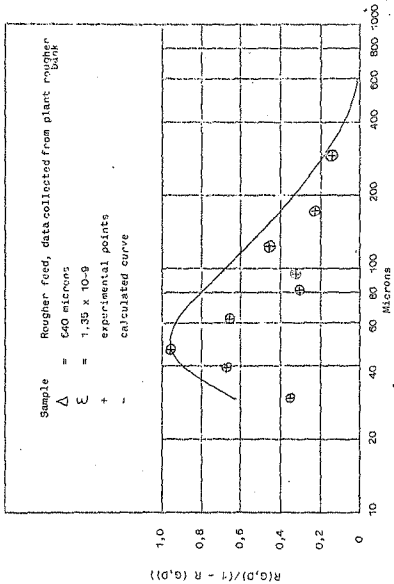


Figure 8a Specific flotation rate constant for apatite as a function of particle size

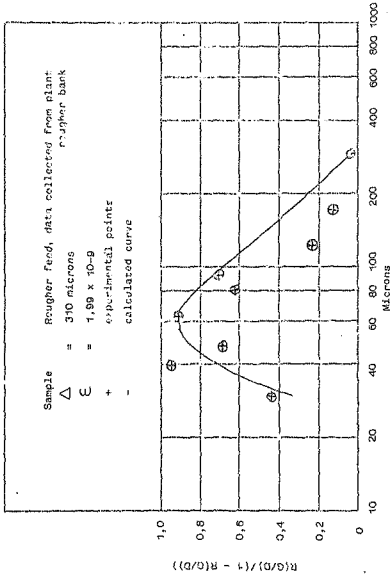


Figure 10 Specific flotation rate constant for gangue as a function of particle size

Assay sieve analysis		Average micron size									
		300	175	124	96	81	63	48	40	30	
Feed	Mass percent	26.4	10.6	8.5	5.1	4.9	5.3	4.7	2.8	31.5	
	Percent apatite	34.28	47.04	46.34	45.39	42.95	39.7	37.35	34.90	31.91	
First concntrate	Mass percent	22.0	18.7	16.8	10.5	8.4	12.1	10.6	7.9	67.9	
	Percent apatite	90.54	90.54	88.65	83.45	83.45	72.58	64.94	60.52	47.52	

Colborn's Function		Average micron size									
		300	175	124	96	81	63	48	40	30	
Apatite	Experimental	0.14	0.23	0.47	0.32	0.30	0.66	0.97	0.68	0.35	
	Calculated	0.19	0.40	0.58	0.73	0.83	0.94	0.07	0.91	0.63	
Gangue	Experimental	0.03	0.11	0.22	0.71	0.62	0.97	0.68	0.95	0.43	
	Calculated	0.02	0.32	0.55	0.72	0.82	0.91	0.86	0.72	0.39	

Table 5 Average assay sieve analysis for rougher feed and first concentrate with the estimated and predicted values of Colborn's function

was then crushed using a jaw crusher to pass an 8 mesh Tyler standard sieve (-2362 $\mu$ ). The sample was thoroughly mixed then split into 1 kg samples. In order to simulate the Feskor flotation process as close as possible in the laboratory, the same steps as those carried out in the plant were observed. These steps are:-

- 1 - rod milling ore
- 2 - copper flotation
- 3 - magnetite removal
- 4 - apatite flotation

A sample of the standard ore (2,5 kg) was loaded into a laboratory rod mill with 1 $\ell$  of industrial water and milled for 300 sec at 80 r.p.m.. The slurry was then transferred to a 5 $\ell$  batch flotation cell, where, using it's back edge as a weir the sample was split through a riffler. The sample was split four successive times to give a split feed sample of approximately 0,187 kg. The remainder was combined to form the feed to the copper float. The slurry was then conditioned for 120 sec. at ambient temperature with potassium amyl xanthate (0,2 kg/t) followed by 60 sec with pine oil (0,02 kg/t). The speed of the impeller during the conditioning period was 2300 r.p.m.. After conditioning the impeller speed was not reduced, as in the case of the standard Feskor laboratory flotation technique, as the concentrate was allowed to flow over the cell lip without the aid of rubber scrapers. The slurry was then made up with industrial water to within 0,7 cm of the cell lip. This was the height rise upon aeration of the pulp. Aeration was started, the volume of air being monitored with a rotameter (4,2 $\ell$ /m). The concentrate was collected over a period of 245 sec,

by which time no more concentrate was coming over the cell lip.

After copper flotation the sides of the cell were washed with industrial water. The magnetite was removed using a hand magnetic separator. When all the magnetite has been removed from the copper tailings, the magnetite was diluted with 250 ml water and again separated, this ensured that any entrained particles in the magnetite were liberated. These entrained particles were then returned to the copper tailings. This pulp was then split three successive times to give a split feed sample for the apatite float. This split feed sample was then screened and each size fraction sent for assay. The non-magnetic copper tailings were then transferred to a 36 batch flotation cell. The slurry was conditioned at 1800 r.p.m. with sodium silicate (2,2 kg/t) for 120 sec at ambient temperature, followed by 120 sec with a tall oil fatty acid (1,1 kg/t) and a polyglycol ether (0,05 kg/t). During this conditioning period, a layer of heavily loaded froth built up on the surface of the slurry and was discharged very rapidly over the froth lip as soon as aeration started, which necessitated a zero time correction to each of the batch experiments. The concentrate was collected in cumulative samples for 150 sec. The first four samples were collected at 15 sec intervals and the last three at 30 second intervals.

The zero-time correction was calculated in the following way; the flow rate of water in the concentrate was plotted as a function of the time at which the sample was taken, and the curve was extrapolated through the second and third points to the time for the first sample. This defined the rate at which water would have been collected had no froth accumulated during the conditioning. The rate of water actually collected compared with its extrapolated rate gave an estimate of the effective flotation time for the first sample, and the origin was adjusted accordingly. Figure 11 shows a typical set of data. The basic data that was used for the estimation of the kinetic parameters was the cumulative recovery of apatite and gangue as a function of time. Figures 12 - 16 show both the computed and experimental data points for the fraction of each mineral that remains in the batch cell.

The theoretical reasoning behind plotting the natural logarithm of the fraction remaining against time is evident from the following consideration. If, as it has been stated, the recovery of the valuable mineral is comparable with a first order chemical reaction, then starting with the first order reaction rate equation

$$-\frac{d(c)}{dt} = k(c)$$

where C is the concentration, the following may be deduced: The rate equation for a first order reaction may be integrated after it has been written in the form

$$-\frac{d(C)}{(C)} = kdt$$

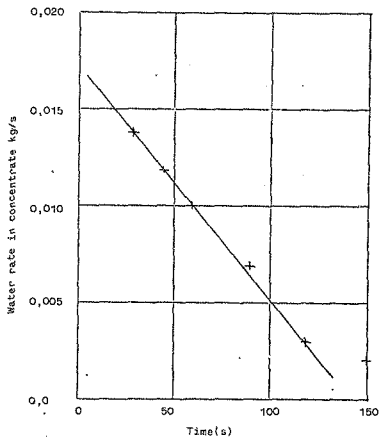


Figure 11 Water rate as a function of sample time in a batch test

Calculation of effective origin:

Water collected - first sample = 0,294 kg  
Water rate in first sample by extrapolation = 0,0178  
Effective time for first sample =  $\frac{0,294}{0,0178}$  = 16,5s

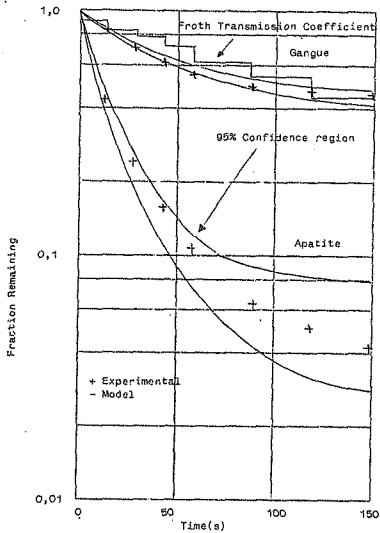


Figure 12 Batch data for experiment P52

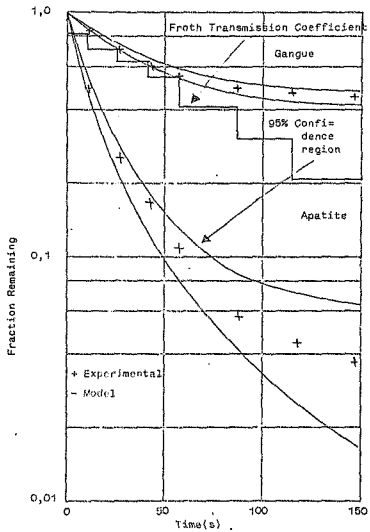


Figure 13 Batch data for experiment P51

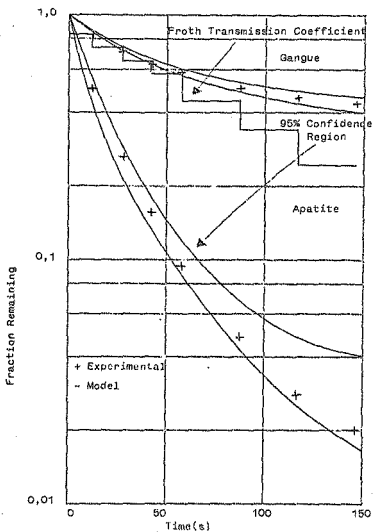


Figure 14 Batch data for experiment P50

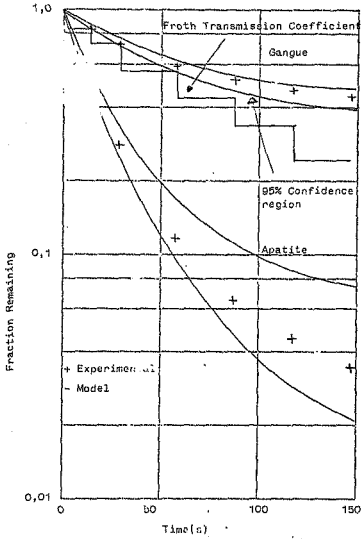


Figure 15 Batch data for experiment P49

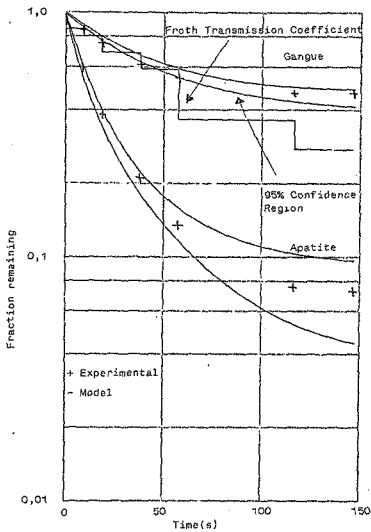


Figure 10 Batch data for experiment P48

If the concentration of C is  $C_1$  at time  $t_1$  and  $C_2$  at  $t_2$ ,

$$- \int_{C_1}^{C_2} \frac{d(C)}{C} = k \int_{t_1}^{t_2} dt$$

$$\ln \frac{C_1}{C_2} = k (t_2 - t_1)$$

At the start of a process  $t_1 = 0$  thus the above equation can be written

$$\ln \frac{C_0}{C} = kt \quad (1)$$

At any time interval the concentration  $C_0$  will be equal to that of the feed (F) and C to that of the tails T. Equation (1) can thus be written

$$\ln \frac{F}{T} = kt \quad (2)$$

The mass balance equation for any process with

C = concentrate

F = feed

T = tails

$$\text{is } F = C + T \quad (3)$$

Also the recovery can be expressed as

$$\frac{F}{2} = \text{Recovery} \quad (4)$$

Substituting equation (3) in equation (2)

$$\ln \frac{F}{R - C} = kt \quad (2a)$$

Substituting equation (4) in equation 2a

$$\ln (1 - \text{Recovery}) = kt$$

Thus the plot of  $\ln (1 - \text{Recovery})$  against time will give a curve whose gradient is equal to the rate constant for the process.

All these curves show the characteristic curve on a log-linear plot, which is an indication of the departure of the process from linear kinetic behaviour. This departure has been ascribed to three possible causes (10): distribution of the rate constant, gradual reduction in the froth production capacity during the course of the experiment, and true non-linear kinetic behaviour. The last of these three possibilities was excluded by Loveday (11). He showed that the average value of the rate constant for all particles was invariant with initial pulp concentration, and so eliminated the multiple-order-rate model. It appears to be impossible to separate in any unambiguous way the effect of decreasing froth production from the effect of rate-constant distribution. During the batch tests, the production of froth could not be maintained for more than about 150 sec. This was due to the pulp level dropping during the test because no water was added and the froth stability decreasing as the amount of solid contained in the froth decreased progressively. The progressive decrease in the production of froth was probably a good indication that a large part of the fall off in flotation rate was due to reduction in the ability of the froth to transmit the solid, that was carried across the pulp interface, over the froth lip. The froth production rate is included in the model through the froth transmission coefficient.

During the batch tests, the water production rate decreased steadily, and consequently the froth transmission coefficient as calculated from the water rate decreased also. The calculated values of the froth transmission coefficient which are shown on figures 12 - 16, were used in the theoretical model for the estimation of the kinetic constants.

The standard regression computer programme (12, 10) that was used in the estimation of the kinetic constants for the gangue and the apatite incorporates all the necessary statistical tests to determine the number of significant values over which the rate constant must be distributed. Earlier work on this ore by Davey(13) and Moys(12) indicated that the apatite and gangue were each characterized by two kinetic parameters; the specific rate constant for the floatable component, and the fraction of unfloatable components. These estimations are shown in figure 17 and table 5a.

#### 3.6.1.2 Conditioned rougher feed

The reagent consumption in the operating plant at Foskor differs from that predicted by batch flotation in the laboratory. Table 6 shows the comparative quantities. In spite of the differences both the plant and the laboratory give the same order of grade and recovery. It was important in the experimental programme to observe the effects of floating conditioned feed on the kinetic parameters.

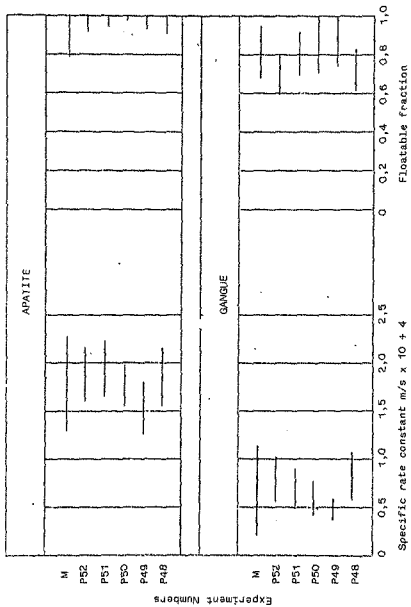


Figure 17 Standard ore 95% confidence limits of parameters, estimated from batch tests

Experiment No.	Component	Specific rate constant m/s x 10 <sup>4</sup>	Nonlinear 95% confidence interval $\times 10^{-4}$	Fraction of floatable compound	Nonlinear 95% confidence interval
P48	Apatite	1,863	-1,57 - 2,15	0,945	0,90 - 0,99
	Gangue	0,627	0,58 - 1,07	0,725	0,62 - 0,83
P49	Apatite	1,499	1,28 - 1,81	0,996	0,93 - 1,0
	Gangue	0,483	0,35 - 0,59	0,957	0,74 - 1,0
P50	Apatite	1,758	1,57 - 1,98	1,0	0,97 - 1,0
	Gangue	0,577	0,41 - 0,76	0,867	0,71 - 1,0
P51	Apatite	1,939	1,67 - 2,24	0,981	0,94 - 1,0
	Gangue	0,708	0,52 - 0,90	0,806	0,69 - 0,92
P52	Apatite	1,892	1,61 - 2,18	0,954	0,92 - 0,99
	Gangue	0,775	0,56 - 0,96	0,674	0,59 - 0,76

Table 5a Kinetic parameters estimated from batch tests on standard ore.

Reagent	Consumption g/t	
	Laboratory	Plant
	110	200
Poly ether	50	50
Sodium silicate	220	600
Sodium hydroxide	-	100

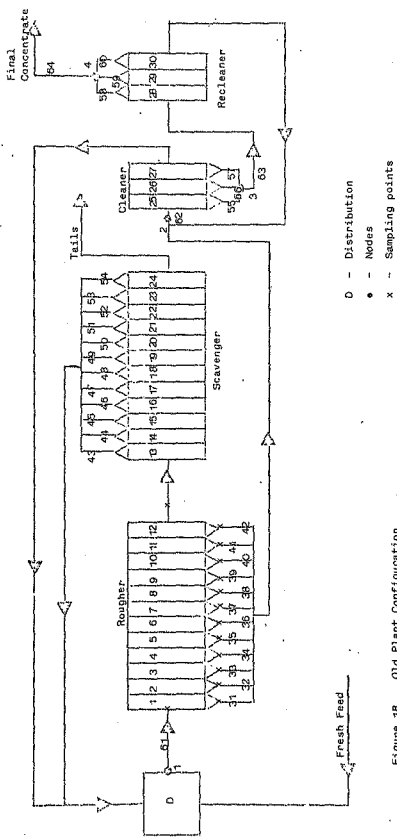
Table G Comparative consumption of reagents in plant and laboratory

Figure 18 shows the old plant lay-out and the sampling points. The reagents are added to the fresh feed before the distributor. The combined recirculating load plus the fresh feed was gravity fed to the first cell of the rougher bank through a vertical standpipe. This stream was cut eight times to obtain a representative sample for the assay sieve analysis and another eight times to give sufficient pulp to carry out a batch flotation test. Table 7 shows a typical assay sieve analysis for the rougher feed.

The conditioned plant rougher feed was brought back to the laboratory and allowed to stand for one hour, this then ensured that the effect of conditioning time was constant for each experiment. The clear water was then syphoned off from the settled pulp, and retained and used to wash the pulp into a 3 litre batch flotation cell. The cell was then filled, using the syphoned water, to within 0,7 cm of the lip. Aeration was started and measured by a rotameter in the air line. The concentrate was collected in cumulative samples for 150 sec., as in the case of the standard ore. The fraction of each mineral that remained in the batch cell was computed and plotted against time for each of the batch experiments. (Figures 19 - 30). The kinetic constants for gangue and apatite are shown in Figure 31 and Table 8.

#### 3.6.1.3 Unconditioned new plant feed

During the period of investigation Foskor



- D - Distribution
- - Nodes
- x - Sampling points

Figure 18 Old Plant Configuration

Average Particle Size (microns)	Mass percent	Percent Apatite
300	27,83	44,97
174	12,04	53,35
124	10,36	47,60
96	6,34	42,70
81	5,51	39,82
63	6,49	37,46
48	4,67	36,41
40	4,39	36,49
30	22,42	35,25

Table 7 Old plant rougher feed assay sieve analysis

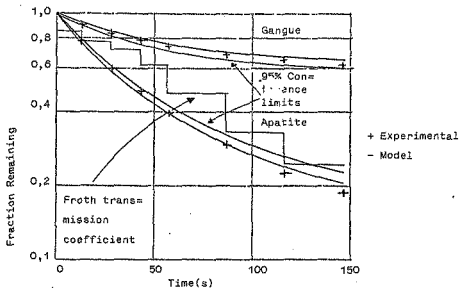


Figure 19 Batch data for experiment RF/16/76

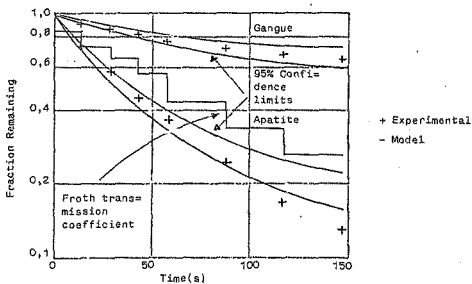


Figure 20 Batch data for experiment RF/15/76

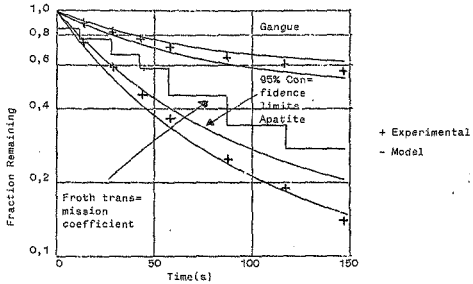


Figure 21 Batch data for experiment RF/14/77

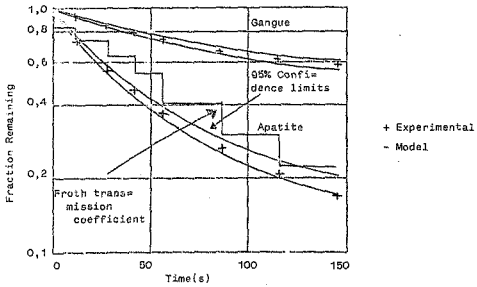


Figure 22 Batch data for experiment RF/13/76

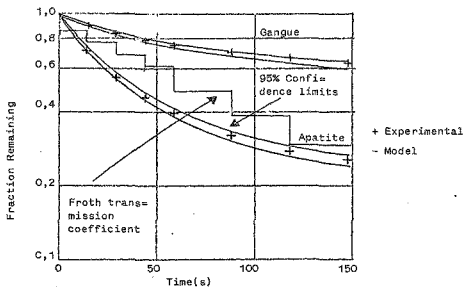


Figure 23 Batch data for experiment RF/10/76

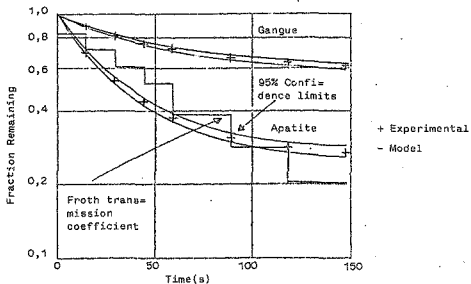


Figure 24 Batch data for experiment RF/9/75

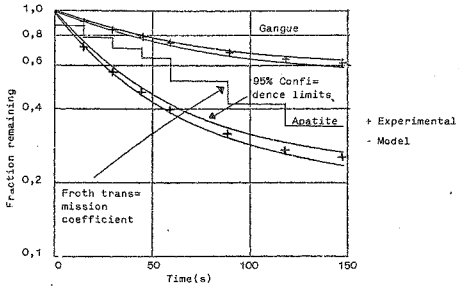


Figure 25 Batch data for experiment RF/8/76

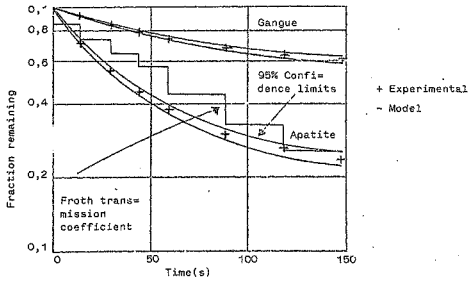


Figure 26 Batch data for experiment RF/7/76

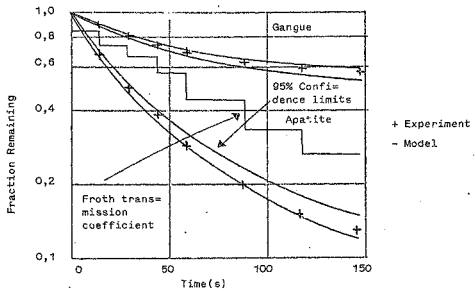


Figure 27 Batch data for experiment RF/6/76

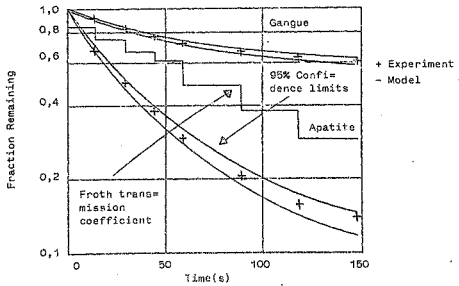


Figure 28 Bath data for experiment RF/5/76

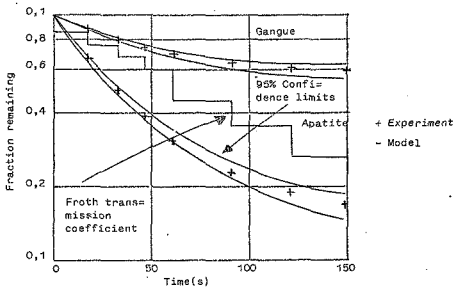


Figure 29 Batch data for experiment RF/4/76

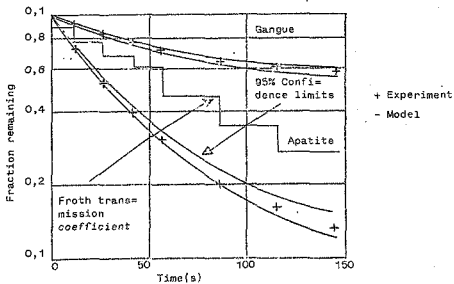


Figure 30 Batch data for experiment RF/3/76

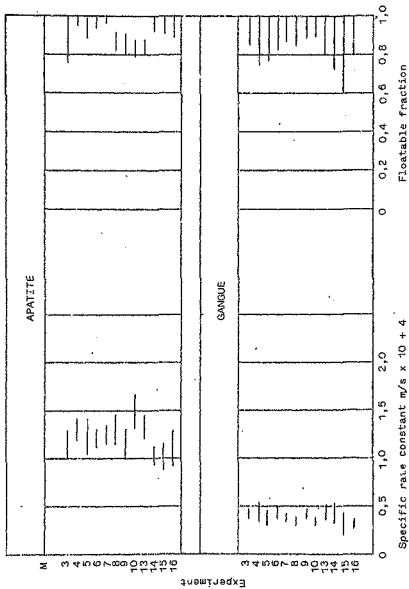


Figure 31 Rougher feed old plant 95% confidence limits of parameters estimated from batch tests

Experiment No.	Component	Specific rate constant m/s x 10 + 4	Nonlinear 95% confidence interval x 10 + 4	Fraction of floatable compound	Nonlinear 95% confidence interval
RF/16/76	Apatite Gangue	0,905 0,285	0,86 - 1,01 0,28 - 0,37	1,0 1,0	0,94 - 1,0 0,78 - 1,0
RF/15/76	Apatite Gangue	1,066 0,280	0,93 - 1,30 0,21 - 0,42	1,0 1,0	0,89 - 1,0 0,60 - 1,0
RF/14/76	Apatite Gangue	0,991 0,367	0,89 - 1,16 0,31 - 0,51	1,0 1,0	0,92 - 1,0 0,72 - 1,0
RF/13/76	Apatite Gangue	1,001 0,383	0,94 - 1,13 0,38 - 0,51	1,0 1,0	0,94 - 1,0 0,78 - 1,0
RF/10/76	Apatite Gangue	1,328 0,307	1,22 - 1,45 0,30 - 0,36	0,82 <sup>c</sup> 1,0	0,80 - 0,86 0,88 - 1,0
RF/09/76	Apatite Gangue	1,497 0,400	1,33 - 1,68 0,38 - 0,47	0,824 1,0	0,79 - 0,85 0,87 - 1,0
RF/08/76	Apatite Gangue	1,168 0,317	1,02 - 1,32 0,30 - 0,38	0,851 1,0	0,81 - 0,89 0,85 - 1,0

Table 8 Kinetic parameters estimated from batch tests on rougher feed

Experiment No.	Component	Specific rate constant m/s x 10 + 4	Nonlinear 95% confidence interval x 10 + 4	Fraction of floatable cut bound	Nonlinear 95% confidence interval
RF/07/76	Apatite Gangue	1,312 0,350	1, 15 - 1,47 0,33 - 0,42	0,868 1,0	0,83 - 0,91 0,86 - 1,0
RF/08/76	Apatite Gangue	1,234 0,410	1, 17 - 1,35 0,39 - 0,51	1,0 1,0	0,86 - 1,0 0,83 - 1,0
RF/08/76	Apatite Gangue	1,157 0,388	1, 11 - 1,31 0,31 - 0,45	0,997 0,942	0,94 - 1,0 0,77 - 1,0
RF/04/76	Apatite Gangue	1,234 0,432	1, 07 - 1,42 0,35 - 0,55	0,954 0,901	0,89 - 1,0 0,74 - 1,0
HF/03/76	Apatite Gangue	1,255 0,383	1, 20 - 1,42 0,37 - 0,48	0,999 1,0	0,95 - 1,0 0,85 - 1,0

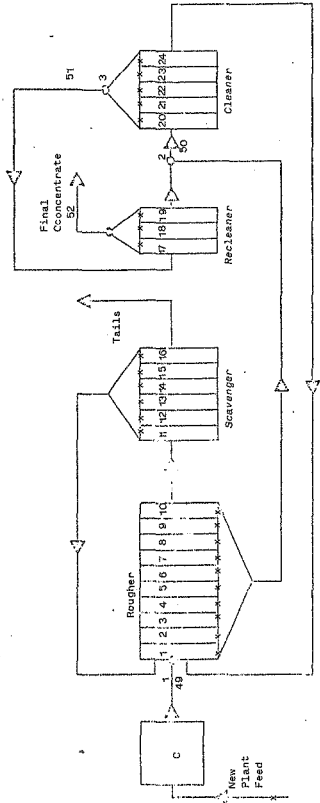
Table 8 continued

changed over from using 50 cubic foot flotation cell for the flotation of foskorite to 300 cubic foot cells. Also new mills were being brought on line to facilitate the expansion in production. This increase in cell size, by a factor of six, and also the fact that the particle size distribution for the new section was markedly different gave rise to a further series of experimental runs.

Colborn's  $\phi(G,D)$  function was assumed to be the same as for the old plant, this for two reasons: the largest particle floated and the  $D_{max}$  value should not vary with increase flow rate (14), which is basically what happens with increased cell volume, the coarseness of grind could possibly effect the coarse end of the  $\phi(G,D)$  curve, but not to a significant extent. The second reason was that the amount of work required to obtain a satisfactory curve was out of all proportion to the information gained.

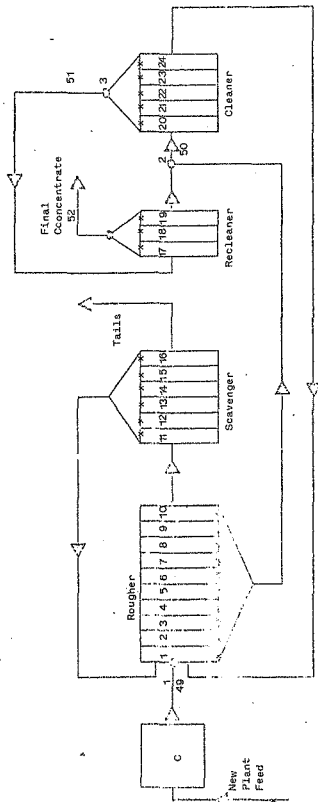
Figure 32 shows the new plant configuration, and sampling points. Unconditioned plant feed was sampled before it entered the conditioning tanks. Enough sample was cut to just fill a 3 litre flotation cell, and a representative sample cut to carry out an assay analysis Table 9. The unconditioned feed sample brought back to the laboratory and tested to find a suitable reagent combination. After finding a reagent combination that gave a satisfactory float an incremental batch flotation was carried out.





C - Conditioning tank  
• - Nodes  
x - Sampling points

Figure 32. New plant configuration



C - Conditioning tank  
• - Nodes  
x - Sampling points

Figure 32 New plant configuration



Average Particle Size (microns)	Mass Percent	Apatite Percent
300	37,01	25,06
174	10,92	33,33
124	9,46	34,52
96	4,79	35,22
81	3,89	35,93
63	4,49	35,93
48	1,30	35,22
40	2,78	35,46
30	25,36	29,55

Table 9      New plant feed assay sieve analysis

Table 10 shows the reagent combinations used. The fraction of each mineral that remains in the cell was plotted against time for each batch experiment (Figures 33 - 43). The kinetic constants for gangue and apatite are shown in Figure 44 and Table 11.

#### 3.6.1.4 Unconditioned P.M.C. tailings

The carbonatite core of the Phalaborwa complex is a low copper bearing deposit which is mined by the Palabora Mining Company. This part of the ore body also contains a significant amount of apatite bearing rock (average 21% apatite). After the copper bearing minerals have been recovered by P.M.C. the tailings are pumped to Foskor and the apatite floated. Due to the reagents used in the recovery of copper and also other contaminants from the P.M.C. gas scrubbing plant, the P.M.C. tailings can not be floated with the same reagents as foskorite.

Samples of unconditioned P.M.C. tailings feed were cut from the receiving station at Foskor, and floated in the same manner as described for the new plant unconditioned feed. The reagent combinations used for this test series are shown in table 12. Due to the regrinding process at P.M.C. the particle size distribution is different to that of both the old and new plant feeds. The assay sieve analysis of P.M.C. tailings feed is shown in Table 13.

Experiment number	Reagent consumption kg/t		
	Sodium silicate	Fatty acid	Polyglycol ether
NPB 1	1,05	0,39	0,07
NPB 2	Experiment terminated		
NPB 3	1,00	0,38	0,06
NPB 4	1,02	0,38	0,06
NPB 5	0,96	0,36	0,06
NPB 6	1,07	0,40	0,07
NPB 7	1,22	0,37	0,06
NPB 8	1,22	0,37	0,06
NPB 9	1,22	0,37	0,06
NPB 10	0,94	0,35	0,12
NPB 11	0,93	0,35	0,12
NPB 12	0,93	0,35	0,12

Table 10 Reagent combination used to float unconditioned  
now plant feed

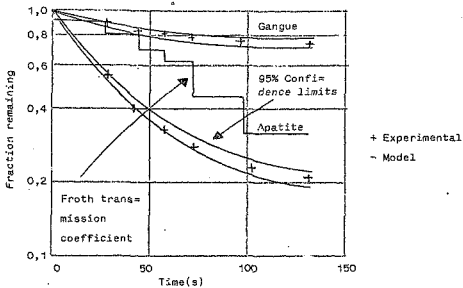


Figure 33 Batch data for experiment NPB 1

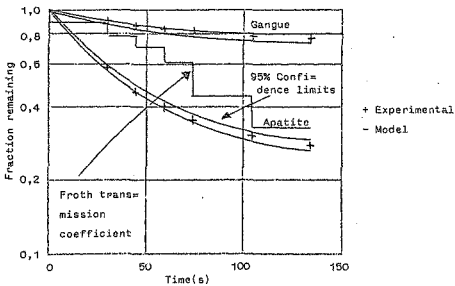


Figure 34 Batch data for experiment NPB 3

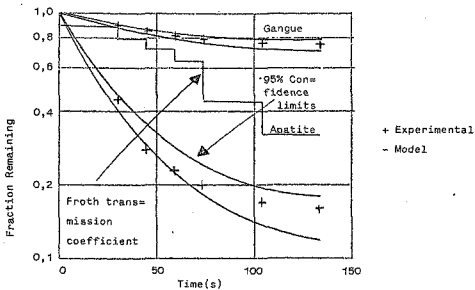


Figure 35 Batch data for experiment NPB 4

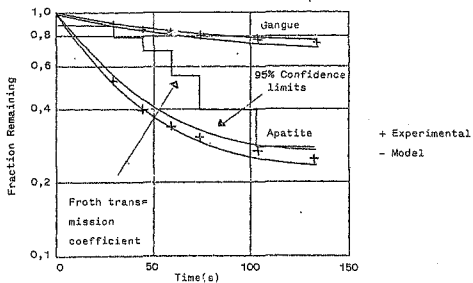


Figure 36 Batch data for experiment NPB 5

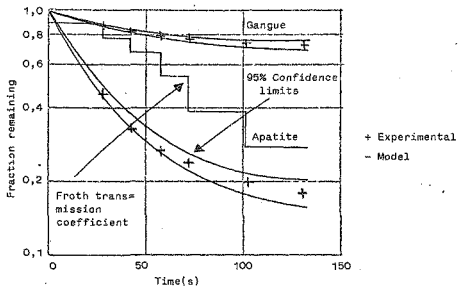


Figure 37 Batch data for experiment NPB 6

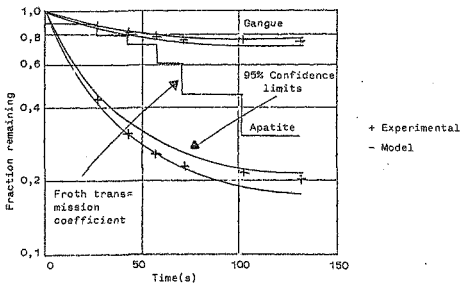


Figure 38 Batch data for experiment NPB 7

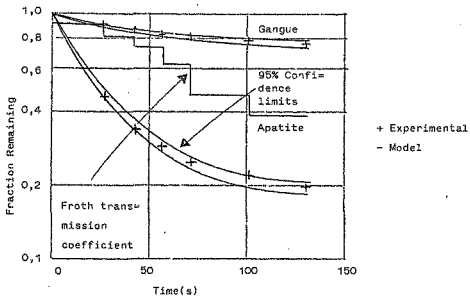


Figure 39 Batch data for experiment NPB 8

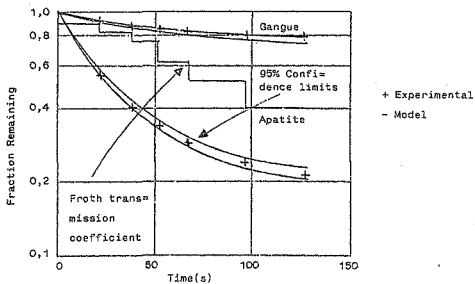


Figure 40 Batch data for experiment NPB 9

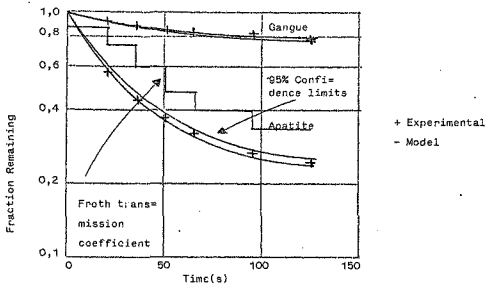


Figure 41 Batch data for experiment NPD 10

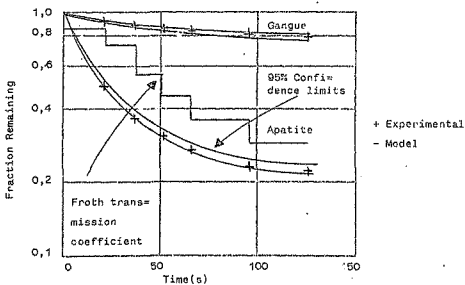


Figure 42 Batch data for experiment NPD 11

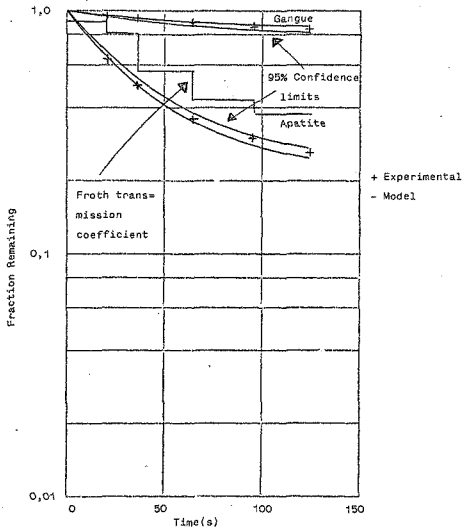


Figure 43 Batch data for experiment NPB 12

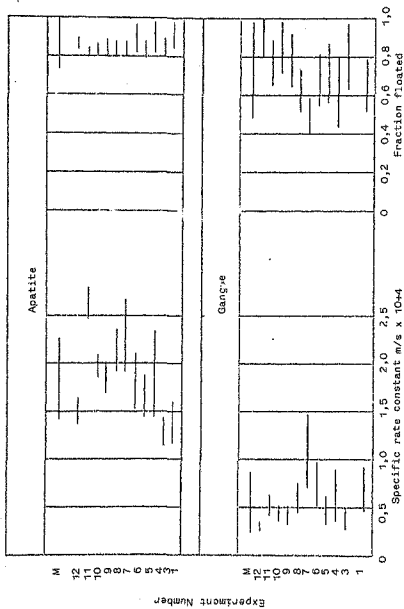


Figure 44 New plant feed 95% confidence limits of parameters estimated from batch tests

Experiment No.	Component	Specific rate constant m/s x 10 <sup>4</sup> + 4	Nonlinear 95% confidence interval= val. m/s x 10 <sup>4</sup>	Fraction of floatable compound	Nonlinear 95% confidence interval.
NPB 1	Apatite	1,384	1,19 - 1,60	0,926	0,87 - 0,98
	Gangue	0,692	0,49 - 0,92	0,659	0,52 - 0,78
NPB 3	Apatite	1,271	1,13 - 1,42	0,853	0,8 - 0,89
	Gangue	0,373	0,28 - 0,47	0,810	0,64 - 0,97
NPB 4	Apatite	1,842	1,45 - 2,33	0,922	0,85 - 0,98
	Gangue	0,615	0,36 - 0,91	0,829	0,43 - 0,80
NPB 5	Apatite	1,638	1,43 - 1,87	0,841	0,80 - 0,88
	Gangue	0,473	0,34 - 0,61	0,718	0,56 - 0,87
NPB 6	Apatite	1,789	1,52 - 2,10	0,903	0,85 - 0,95
	Gangue	0,736	0,52 - 0,98	0,676	0,54 - 0,80
NPB 7	Apatite	2,248	1,91 - 2,67	0,837	0,80 - 0,87
	Gangue	1,053	0,71 - 1,46	0,491	0,40 - 0,57
NPB 8	Apatite	2,104	1,91 - 2,33	0,847	0,82 - 0,87
	Gangue	0,595	0,45 - 0,76	0,624	0,51 - 0,73

Table 11 Kinetic parameters estimated from batch tests on new plant feed

Experiment No.	Component	Specific rate constant m/s x 10 <sup>4</sup> + 4	Nonlinear 95% confidence interval val m/s x 10 <sup>4</sup>	Fraction of floatable compound	Nonlinear 95% confidence interval
NPB 9	Apatite Gangue	1,825	1,68 - 1,98	0,852	0,83 - 0,87
		0,406	0,31 - 0,50	0,790	0,65 - 0,93
NPB 10	Apatite Gangue	1,962	1,85 - 2,08	0,844	0,83 - 0,86
		0,429	0,35 - 0,51	0,852	0,72 - 0,98
NPB 11	Apatite Gangue	2,621	2,46 - 2,79	0,838	0,82 - 0,85
		0,518	0,42 - 0,62	0,763	0,65 - 0,88
NPB 12	Apatite Gangue	1,484	1,36 - 1,61	0,867	0,84 - 0,90
		0,267	0,24 - 0,33	1,0	0,80 - 1,0

Table 11 continued

Experiment number	Reagent consumption kg/t			
	Sodium meta-silicate	Natural Poly-saccharide	Fatty acid	Polyglycol ether
PMC 1	2,11	1,13	0,42	0,14
PMC 2	2,13	1,14	0,43	0,14
PMC 3	2,14	1,14	0,43	0,14
PMC 4	0,69	1,10	0,41	0,07
PMC 5	0,70	1,12	0,42	0,07
PMC 6	0,70	1,12	0,42	0,07
PMC 7	2,77	1,11	0,42	0,14
PMC 8	2,76	1,10	0,28	0,07
PMC 9	2,73	1,09	0,41	0,07
PMC 10	2,14	1,14	0,43	0,07
PMC 11	2,13	1,13	0,43	0,07
PMC 12	2,13	1,13	0,43	0,07

Table 12 Reagent combination used to float unconditioned P.M.C. tailings feed

Average Particle size (microns)	Mass Percent	Apatite Percent
300	7,76	9,2
174	11,54	15,8
124	13,45	20,8
96	8,48	23,2
81	5,31	23,9
63	7,70	24,3
48	5,61	24,1
40	3,38	22,5
30	36,76	18,0

Table 13 P.M.C. tailings feed assay sieve analysis

Again Colborn's  $\theta(G,D)$  function was assumed to be the same for the old plant rougher feed for similar reasons as those given for the new plant unconditioned feed, excepting that fineness of grind could possibly effect the fine fraction end of the  $\theta(G,D)$  curve. The kinetic constants for gangus and apatite are shown in Figure 45 and Table 14.

### 3.6.2. Continuous flotation

#### 3.6.2.1 Old plant

The estimation of kinetic parameters from a continuous operating plant requires only data from the rougher bank, as one of the criteria of the simulator is that the material will float at the same rate in every stage, and only the amount recovered will vary with stage: i.e. the holding time varies. To facilitate the ease of naming the streams and stages of a large plant unambiguously the following numbering system has been adopted (15). Let the stages be numbered 1 to N where N is the total number of stages. Then the tailing stream is also numbered 1 to N, the concentrate stream is numbered N + J where J is the number of the stage from which it emanates. Let any streams that arise from a node be labled 2N+K where K is the number of the node. The feed stream is unnumbered. Figure 18 shows the old plant plan view using this numbering system.

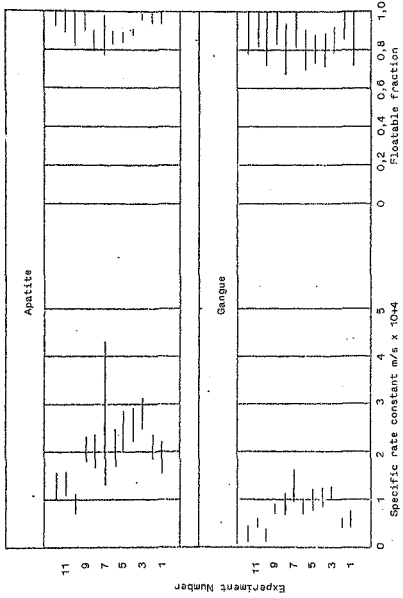


Figure 45 P.M.C. tails feed 95% confidence limits of parameters estimated from batch tests

Experiment Number	Component	Specific rate constant m/s x 10 <sup>4</sup> ± 4	Non linear 95% confidence interval val m/s x 10 <sup>4</sup>	Fraction of floatable compound	Non linear 95% confidence interval
PMC 1	Apatite	2,216	1,82 - 2,90	0,984	0,94 - 1,0
	Gangue	0,775	0,58 - 0,99	0,855	0,72 - 0,99
PMC 2	Apatite	2,449	2,23 - 2,91	0,985	0,95 - 1,0
	Gangue	0,600	0,57 - 0,73	1,0	0,85 - 1,0
PMC 3	Apatite	3,423	3,13 - 3,85	0,991	0,97 - 1,0
	Gangue	1,453	1,26 - 1,65	0,845	0,78 - 0,90
PMC 4	Apatite	3,149	2,76 - 3,61	0,893	0,87 - 0,92
	Gangue	1,350	1,14 - 1,56	0,794	0,72 - 0,87
PMC 5	Apatite	2,994	2,58 - 3,51	0,876	0,85 - 0,89
	Gangue	1,282	1,07 - 1,90	0,808	0,73 - 0,88
PMC 6	Apatite	2,539	2,12 - 3,07	0,871	0,84 - 0,90
	Gangue	1,039	0,83 - 1,26	0,804	0,70 - 0,90
PMC 7	Apatite	2,974	1,64 - 5,39	0,894	0,78 - 0,88
	Gangue	1,519	1,20 - 2,08	1,00	0,82 - 1,0

Table 14. Kinetic parameters estimated from batch tests on P.M.C. tailings feed

Experiment Number	Component	Specific rate constant $m/s \times 10^{-4}$	Non linear 95% confidence interval val $m/s \times 10^{-4}$	Fraction of floatable compound	Non linear 95% confidence interval
PAC 8	Apatite Gangue	2,511 1,088	2,15 - 2,91 0,84 - 1,35	0,854 0,805	0,80 - 0,90 0,67 - 0,83
PAC 9	Apatite Gangue	2,511 0,9189	2,25 - 2,87 0,87 - 1,12	0,967 1,00	0,81 - 1,0 0,83 - 1,0
PAC 10	Apatite Gangue	1,069 0,3567	0,88 - 1,38 0,31 - 0,48	0,951 1,00	0,83 - 1,0 0,72 - 1,0
PAC 11	Apatite Gangue	1,604 0,5778	1,36 - 1,98 0,52 - 0,73	0,969 1,0	0,89 - 1,0 0,82 - 1,0
PAC 12	Apatite Gangue	1,604 0,4326	1,44 - 1,99 0,38 - 0,56	1,0 1,0	0,83 - 1,0 0,77 - 1,0

Table 14 continued

Stream 61 was sampled to obtain the necessary feed input data i.e. assay screen analysis Table 7. Streams 31 - 42 were sampled with a sample cutter which covered the complete cell lip. The concentrate flow rate from each stream was measured by allowing the concentrate to flow from the sample cutter into a bucket for a known time, weighing the bucket both full and empty then weighing the dry solid. From this the percent solids and water flow rate was determined per stream. To calculate the mass flow of the feed stream 61 to the rougher bank it was necessary to sample stream 12 (rougher tails) and the combined concentrate stream. Thus from the assay screen analysis of the feed, concentrate and tails of the rougher bank it was possible to calculate the mass flow of the feed to the rougher bank.

Colborn's function  $\phi$  (G,D) that was used in the escimator was that obtained from the work carried out on the conditioned rougher batch test series. The aeration rate for each stage was measured using a rotameter Figure 46. The kinetic constants for gangue and apatite are shown in Figure 47 and Table 15.

#### 3.6.2.2 New plant

Figure 32 gives a plan view of the new plant configuration. Streams 25 to 30 were sampled and their mass flow measured in the same manner as for the old plant. The aeration of the cells was

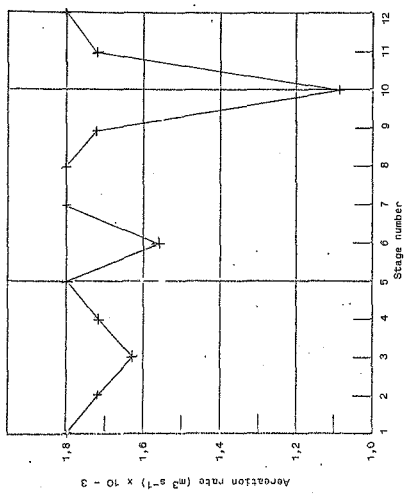


Figure 46 Aeration rate for each stage of the rougher bank in the old plant

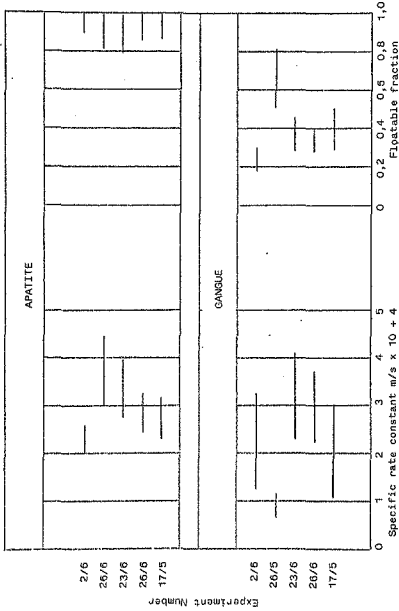


Figure 47 Old plant 95% confidence limits of parameters estimated from continuous runs

Experiment Number	Component	Specific rate constant $m/s \times 10^{-4}$	Non linear 95% confidence interval $m/s \times 10^{-4}$	Fraction of floatable compound	Non linear 95% confidence interval
17 5 76	Apatite Gangue	3,209	2,82 - 3,09	1,00	0,88 - 1,0
		2,275	1,36 - 3,37	0,416	0,30 - 0,92
26 6 76	Apatite Gangue	3,334	3,04 - 4,07	1,00	0,87 - 1,0
		3,328	2,78 - 4,61	0,378	0,29 - 0,41
23 6 76	Apatite Gangue	3,810	3,48 - 4,91	1,00	0,80 - 1,0
		3,599	2,86 - 5,12	0,409	0,29 - 0,47
26 5 76	Apatite Gangue	4,387	3,75 - 5,04	0,919	0,83 - 1,0
		1,148	0,87 - 1,43	0,667	0,52 - 0,81
2 6 76	Apatite Gangue	2,698	2,52 - 3,21	1,0	0,90 - 1,0
		2,672	1,82 - 4,03	0,246	0,18 - 0,30

Table 15 Kinetic parameters estimated from continuous runs carried out on the old plant

measured using an anemometer. Figure 48 shows the aeration rate down the whole bank. Due to the pipe configuration it was impossible to take a sample of either the rougher feed or tails. It was assumed that the assay sieve analysis of the plant feed very closely represented that of the rougher feed, therefore the plant feed was sampled Table 9. The calculation of the mass flow of material into the rougher was obtained from the daily work sheets produced by Foskor, which give the plant feed mass per day. The recirculating load was calculated on the basis of a Foskor report (16) issued by it's engineering department. This stated that the recirculating load was 100% of the flotation feed. The kinetic constants for gangue and apatite are shown in Figure 49 and Table 16

### 3.7

#### Discussion of Kinetic Parameters

##### 3.7.1 Standard Ore

The validity of the kinetic parameters generated by the regression programme can be assessed by the goodness of fit between the experimental and predicted data points. As with any experimental procedure there are random variables associated with the experiment, thus the real test of any predictions generated by a model are the 95% confidence limits.

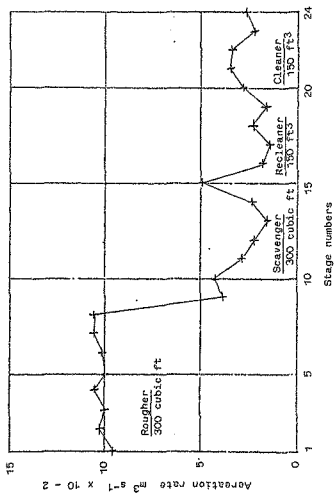


Figure 48 Aeration rate for each stage in the new plant

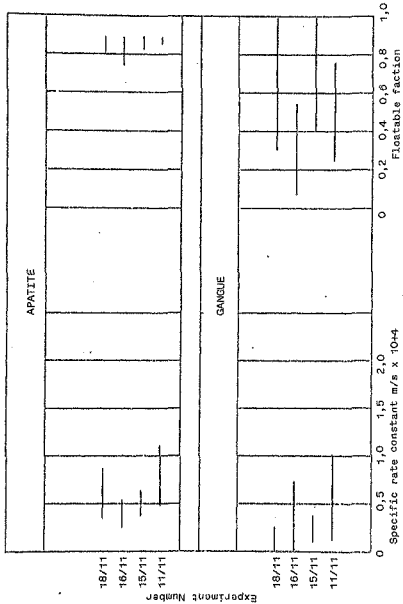


Figure 49 New plant 95% confidence limits of parameters estimated from continuous runs

Experiment Number	Component	Specific rate constant $m/s \times 10 + 4$	Non linear 95% confidence interval $m/s \times 10 + 4$	Fraction of floatable compound	Non linear 95% confidence interval
11/11	Apatite	0,717	0,49 - 1,11	1,0	0,86 - 1,0
	Gangue	0,479	0,14 - 1,01	0,565	0,26 - 0,76
15/11	Apatite	0,475	0,40 - 0,63	1,0	0,84 - 1,0
	Gangue	0,215	0,11 - 0,36	0,800	0,42 - 1,0
16/11	Apatite	0,356	0,26 - 0,54	1,0	0,75 - 1,0
	Gangue	0,321	0,04 - 0,74	0,368	0,08 - 0,55
18/11	Apatite	0,548	0,37 - 0,89	1,0	0,81 - 1,0
	Gangue	0,137	0,06 - 0,26	1,0	0,31 - 1,0

Table 16 Kinetic parameters estimated from continuous tests carried out on the new plant

Experiment Number	Component	Specific rate constant m/s. x 10 + 4	Non linear 95% confidence interval m/s x 10 + 4	Fraction of fluctable component	Non linear 95% confidence interval
11/11	Apatite Gangue	0,717 0,479	0,49 - 1,11 0,14 - 1,01	1,0 0,585	0,85 - 1,0 0,26 - 0,76
15/11	Apatite Gangue	0,475 0,215	0,40 - 0,63 0,11 - 0,36	1,0 0,800	0,84 - 1,0 0,42 - 1,0
16/11	Apatite Gangue	0,356 0,221	0,26 - 0,54 0,04 - 0,74	1,0 0,366	0,75 - 1,0 0,08 - 0,95
18/11	Apatite Gangue	0,548 0,137	0,37 - 0,89 0,06 - 0,26	1,0 1,0	0,81 - 1,0 0,31 - 1,0

Table 16 Kinetic parameters estimated from continuous tests carried out on the new plant

Figures 12 - 16 show that the experimental data points fall within the 95% confidence limits as predicted by the model.

Each of the five batch tests on the standard ore was a replicate, thus in the ideal situation, where no other factors, except those generated by the experiment were allowed, the estimated kinetic parameters should be the same for each of the tests: in practice this is found not to be the case. Figure 17 shows the 95% confidence limits for each of the parameter estimates for apatite and gangue. The specific rate constants for apatite show a degree of overlap, and this would tend to indicate that the "true" specific rate constant value for apatite lies at the mid point of the maximum overlap. The degree of overlap for the specific rate constant for gangue is not so great, as in the case of the apatite, but it can be argued that it is in this overlap region that the true specific rate constant lies.

The amount of material that is floated by the mineral/gangue with a specific rate constant is more difficult to determine because of the physical barrier imposed on the parameter, i.e. it cannot be greater than unity. For this reason the 95% confidence limits are truncated at 1.0, thus the region of overlap is difficult to estimate.

From the parameter estimates it is possible to calculate a 95% confidence band using the mean values of all the five parameters, this gives rise to the 'M' band on figure 17. The M band is calculated on the assumption that the population is normal but with an unknown variance and known mean. It is known (20) that when sampling from a normal distribution with a known mean  $\mu$  and unknown variance that the random variable

$$\frac{\bar{x} - \mu}{s/\sqrt{n}}$$

has a t-distribution with  $n - 1$  degrees of freedom ( $s$  is the standard deviation,  $n$  is the sample size). Thus it follows that

$$P \left[ -t_{\alpha/2} < \frac{\bar{x} - \mu}{s/\sqrt{n}} < t_{\alpha/2} \right] = 1 - \alpha$$

where  $t_{\alpha/2}$  represents the upper  $\alpha/2$  point of the t-distribution.

It can be shown that the above probability statement is equivalent to

$$P \left[ \bar{x} - t_{\alpha/2} \frac{s}{\sqrt{n}} < \mu < \bar{x} + t_{\alpha/2} \frac{s}{\sqrt{n}} \right] = 1 - \alpha$$

And an exact 100  $(1 - \alpha)$  percent confidence interval for  $\mu$  is given by

$$\left( \bar{x} - t_{\alpha/2} \frac{s}{\sqrt{n}}, \bar{x} + t_{\alpha/2} \frac{s}{\sqrt{n}} \right)$$

where  $\bar{x}$  is the mean of the sample.

This M band shows the spread of the specific rate constant and the fraction floated, thus by using

the upper and lower limits of this confidence region it should be possible to predict a band of results within which the experimental results should fall. The width of this confidence band is indicative of the difficulty in estimating a unique value for any of the kinetic parameters. The causes of the band width can be categorized as follows: (a) experimental techniques, (b) experimental parameters, such as small variations in aeration, conditioning time, reagent addition and grinding. The error due to experimental technique is very small and random, because of the care that was taken to perfect a standard technique. The experimental parameters introduce a large variety of errors, the main one being conditioning time, not only of the pulp with the reagents but also the aging of the pulp without any reagents. An effort was made to minimize all the types of errors, but because of the statistical nature of the material being studied, the 95% confidence band is broad.

### 3.7.2 Conditioned rougher feed

Figure 31 shows the 95% confidence bands of each individual experiment. The specific rate constant bands for apatite and gangue show a much narrower width than with the standard ore experiments. This is due, in the main, to there being a much longer conditioning period ca 60 - 90 minutes compared with 3 - 5 minutes for the standard ore. In each rougher

feed test the reagent combination varied, because of normal plant operation. No figures could be obtained from the plant on an hourly basis, but it was noted that the operators on the plant varied the reagent combination and dosage throughout the day. From this it can be concluded that the longer the conditioning time the better the experimental results, as observed by the narrowness of the confidence bands.

Although there is a narrowing of the band width there is still a spread of results, this is especially noticeable in the case of the specific rate constant for apatite. Using the mean values of the kinetic parameters it was possible to calculate the 95% confidence limits on the predicted values. These are represented on figure 31, by the M bands.

### 3.7.3 Batch tests on new plant feed

Unlike the batch tests carried out on the old plant rougher feed, the new plant feed had no reagents added to it, and reagent combinations had to be worked out for each experiment by carrying out several preliminary float tests before arriving at the "best" combination. The main features of the estimated kinetic parameters of the batch tests on the new plant are that the specific rate constant for apatite shows a marked degree of variation with a

corresponding large 95% confidence band. Also the specific rate constant for the gangue has a wide range of values, which is uncharacteristic, as the model has shown that it's prediction of the gangue kinetic constants is better than that for the valuable mineral.

The calculated 95% confidence bands based on the mean value of the kinetic parameters, as shown by the M bands on figure 44, are wide in comparison to the number of experiments carried out. It would be expected that by increasing the number of tests there would be a tendency for any randomness in the experimental procedure to cancel out, thus producing a narrow confidence band. Since this is not the case, there must be other factors influencing the prediction of the kinetic parameters, namely the reagent combination, because it is this that effects the kinetics of the float.

#### 3.7.4 Batch tests carried out on P.M.C. tailings feed

The kinetic parameters estimated for the P.M.C. tailings feed (figure 45) show the same type of deviation in the mean values and 95% confidence limits as for the new plant unconditioned feed. The reasons for this variation in kinetic parameters can be attributed to the same reasons as stated above.

### 3.7.5 Continuous runs, old and new plants

Figures 47 and 49 show the kinetic parameters as estimated for the continuous old and new plants respectively. Again it will be noticed that the confidence bands are wide, this is due to the difficulty in obtaining reliable data from a continuous operating plant. In a small scale environment such as batch flotation in the laboratory or pilot plant work, the experimental parameters are determined or at least under the control of the experimenter, but in the case of a real operating plant it must be accepted that the plant condition is a factor that is not under a unique controller. For example during a sampling programme, that may take from 1 - 2 hours, the type of ore might change, mass feed to the mills or reagent combinations could vary, all of which effect the reproducibility of any given experiment. Also to contend with is the fact that the mass volumes and flow rates are all subject to mechanical variation in the form of pump surges.

It is because of these factors that the confidence limits are so wide. In spite of this there is overlap of the confidence limits which is evidence that the kinetic parameters lie in the boundaries of maximum overlap.

3.7.6 Mean kinetic parameters

For all six types of experiment:

- 1) batch flotation of standard ore
- 2) batch flotation of old plant conditioned rougher feed
- 3) continuous old plant
- 4) batch flotation of new plant unconditioned plant feed
- 5) continuous new plant
- 6) batch flotation of unconditioned P.M.C. tailings feed.

A mean value of the kinetic parameters was calculated with a 95% confidence interval, M-band, (Table 17, figure 50).

It is clear from Figure 50 that there is a wide variation in specific rate constants for apatite, and to a lesser extent for gangue, also the fraction floated for gangue is less well defined than for apatite. Series 1, 4, 6, that is the batch flotation of unconditioned feeds show a good degree of overlap for all parameters, while the batch flotation of the conditioned rougher feed has a small 95% confidence region for the specific rate constants, they are outside the overlap region for apatite and gangue. Both of the continuous tests show a marked deviation from the batch test kinetic parameters, in the case of the old plant the specific rate constant is greater by a factor of 2 and the new plant less by a factor of 0,5, the corresponding fractions floated also show a similar discrepancy. The reasons

Test type	Series	No. of expts.	Component	Specific rate constant m/s x 10 <sup>4</sup>	Non linear 95% confidence interval m/s x 10 <sup>4</sup> + 4	Fraction of floatable compound	Non linear 95% confidence interval
Batch	Standard	5	Apatite	1,70	2,315 - 1,276	0,975	1,0 - 0,781
	Ore (1)		Gangue	0,670	1,4 - 0,200	0,800	0,945 - 0,667
Batch	Old plant conditioned	12	Apatite	1,18	1,293 - 1,056	0,944	1,0 - 0,768
	Rougher Feed (2)		Gangue	0,357	0,501 - 0,198	0,987	1,0 - 0,874
Contin-uous	Old Plant (3)	5	Apatite	3,82	4,48 - 2,495	0,988	1,0 - 0,747
			Gangue	2,86	3,825 - 1,363	0,494	0,908 - 0,600
Batch	New Plant unconditioned	11	Apatite	1,84	2,256 - 1,411	0,865	0,990 - 0,742
	Plant Feed (4)		Gangue	0,560	0,872 - 0,247	0,728	0,976 - 0,480
Contin-uous	New Plant	4	Apatite	0,52	1,142 - 0,084	1,0	1,00
			Gangue	0,288	0,900 - 0,354	0,663	1,0 - 0,153
Batch	PMC Tailings unconditioned	12	Apatite	2,42	2,952 - 1,868	0,936	1,0 - 0,788
	Plant feed		Gangue	0,949	1,353 - 0,545	0,904	1,0 - 0,708

Table 17 Comparison of mean rate constants with their 95% confidence limits (M bands)

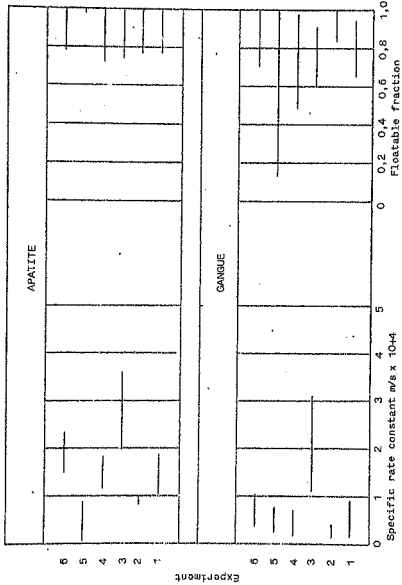


Figure 50 95% confidence limits of mean kinetic parameters

behind these differences in kinetic parameters, for what is, for all purposes the same ore is difficult to resolve. The obvious factors such as fineness of grind with the associated liberation of minerals does not appear to have had any effect upon the kinetic parameters (series 1, 4, 6) because P.M.C. tailings feed is ground much finer than either the standard ore or the new plant feed. (Figure 7)

It is possible to postulate that the kinetic parameters are a function of reagent combination and addition rate, and because these are known and controlled in the batch flotation of the unconditioned feeds, the parameter estimates obtained are similar. In the case of the conditioned rougher feed of the old plant (series 2) the length of conditioning time was the overriding factor in determining the kinetic constants, this would account for the specific rate constants being lower than for the other batch tests as all the reagents had been adsorbed onto the mineral surface.

For both of the continuous series the errors introduced by the system itself contributed to the variation in kinetic constants. Had it been possible to sample the plant at one instant in time the results would have probably been more coherent although not necessarily the same as for the batch test work.

CHAPTER 4.

SIMULATION OF THE FOSKOR PLANT

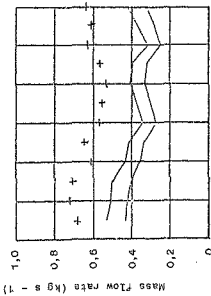
4.1 Simulation of the old plant rougher bank

The ultimate test of any simulator is its usefulness in the prediction of the performance of a continuously operating plant. Since the kinetic parameters from the batch test work on the standard ore, conditions of rougher feed, and the continuous plant were so divergent, all three sets of kinetic parameters were used in estimating the plant performance.

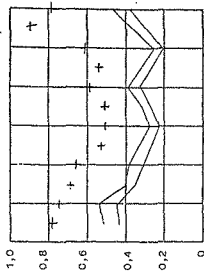
A significant source of uncertainty in the model is the value of the froth transmission coefficient ( $\gamma$ ) in each of the cells.  $\gamma$  was calculated as the ratio of the measured water rate in the concentrate stream to the maximum water production rate. This was consistent with the method used for the estimation of the flotation parameters from the batch tests. The value of  $\gamma$  as calculated from the water ratio is only an estimate of its true value, and a more realistic argument is to let its value lie between the water ratio and unity. Thus in the simulations carried out, both the water ratio and unity values of  $\gamma$  were used.

The simulator FLOAT was used to predict the old plant rougher bank. The 95% confidence regions around the predictions that were generated by the 95% confidence limits in the parameter estimates are shown in figures 51 - 78. The two variables plotted were the percent apatite and mass flow rate in each concentrate stream. These were chosen because they could be directly measured, and did not involve any multiplication of errors, such as recovery which is calculated from two observed variables.

17/5/76



18/5/76



+ Experimental

- 95% Confidence  
limits

96

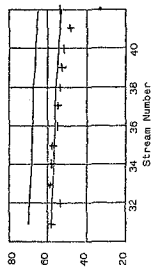
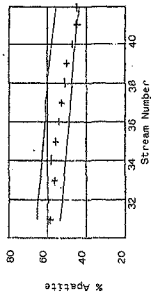
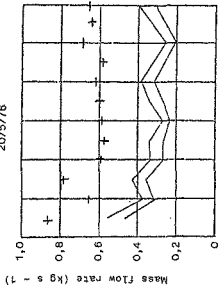


Figure 51

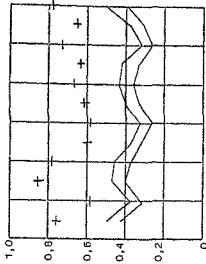
Simulation of old plant kinetic parameters, standard one. Gamma calculated from water ratio

Figure 52 Simulation of old plant kinetic parameters, standard one. Gamma calculated from water ratio.

20/5/76



25/5/77



+ Experimental  
- 96% Confidence limits

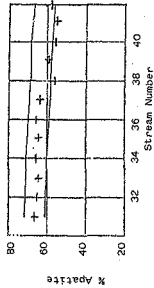


Figure 53  
Simulation of old plant kinetic parameters, standard ore. Gamma calculated from water ra io

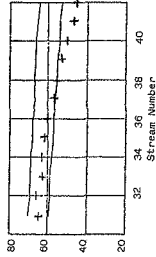
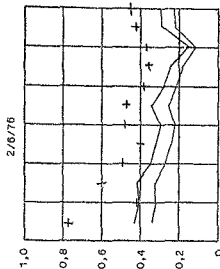
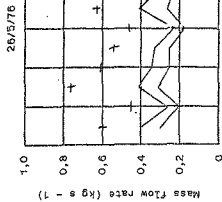


Figure 54  
Simulation of ld plant kinetic parameters, standard ore. Gamma calculated from water ratio.



+ Experimental  
 ~ 95% Confidence  
 Limits

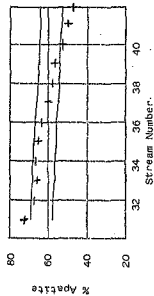


Figure 55 Simulation of old plant kinetic parameters, standard ore. Gamma calculated from water ratio.

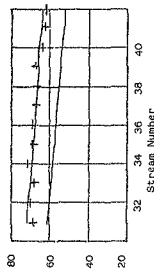
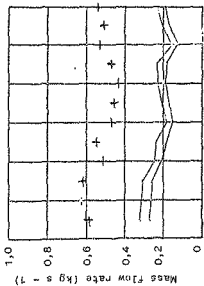
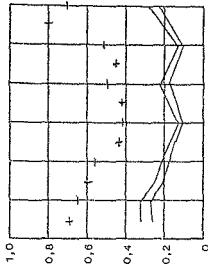


Figure 56 Simulation of old plant kinetic parameters, standard ore. Gamma calculated from water ratio.

17/5/76



18/5/76



+ Experimental

- 95% Confidence limits

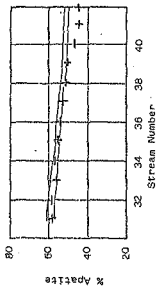


Figure 57 Simulation of old plant kinetic parameters, standard ore. Gamma calculated from water ratio

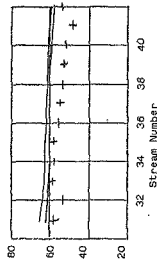


Figure 58 Simulation of old plant kinetic parameters, standard ore. Gamma calculated from water ratio

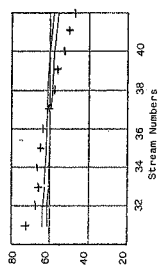
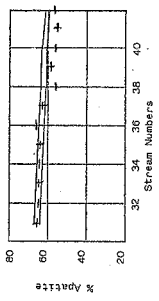
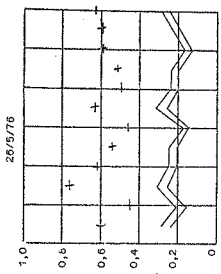
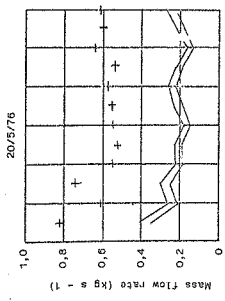


Figure 59 Simulation of old plant kinetic parameters, standard ore. Gamma calculated from water ratio

Figure 60 Simulation of old plant kinetic parameters, standard ore. Gamma calculated from water ratio

+ Experimental  
- 95% Confidence limits

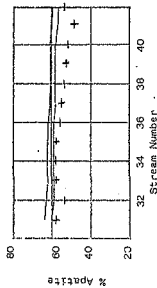
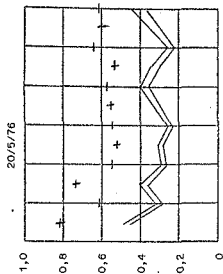
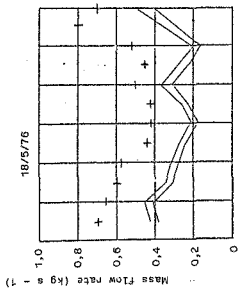


Figure 61 Simulation of old plant kinetic parameters, standard ore. Gamma calculated from water ratio

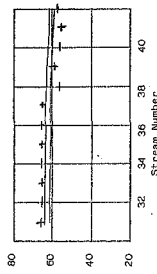
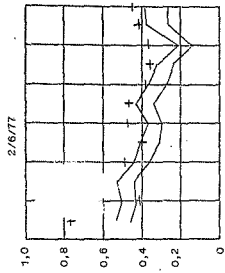
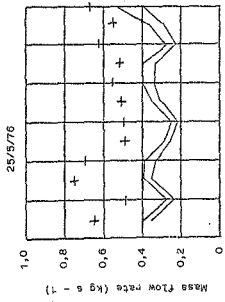


Figure 62 Simulation of old plant kinetic parameters, standard ore. Gamma calculated from water ratio

+ Experimental

- 95% Confidence limits



+ Experimental  
- 95% Confidence  
limits

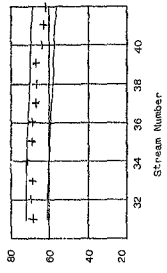
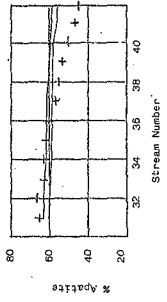
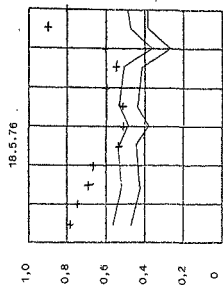
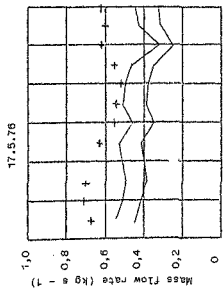


Figure 63 Simulation of old plant kinetic parameters, standard ore. Gamma calculated from water ratio

Figure 71 Simulation of old plant kinetic parameters, standard ore. Gamma calculated from water ratio...



+ Experimental  
- 95% Confidence limits

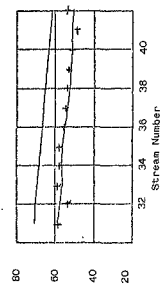
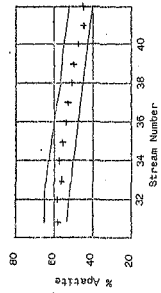


Figure 65 Simulation of old plant Kinetic parameters, standard one Gamma unity

Figure 66 Simulation of old plant Kinetic parameters, standard one Gamma unity

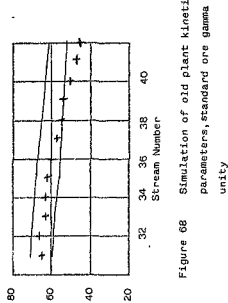
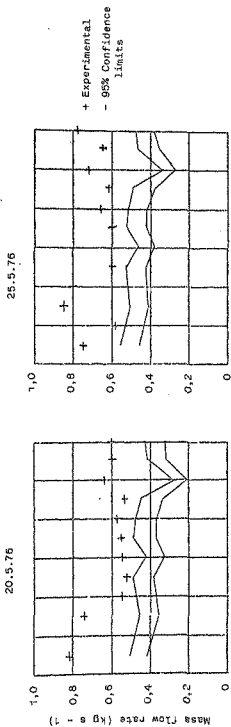


Figure 67 Simulation of old plant kinetic parameters, standardized gamma unity

Figure 68 Simulation of old plant kinetic parameters, standardized gamma unity

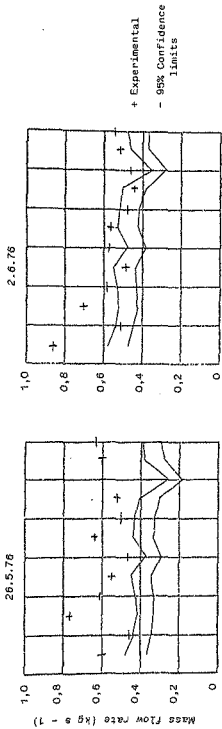


Figure 69 Simulation of old plant kinetic parameters, standard ore. Gamma unity

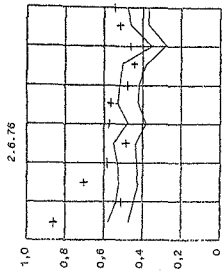


Figure 70 Simulation of old plant kinetic parameters, standard ore. Gamma unity

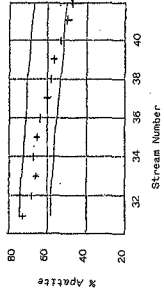


Figure 68 Simulation of old plant kinetic parameters, standard ore. Gamma unity

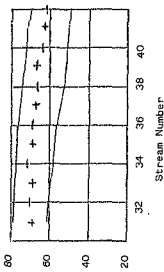


Figure 70 Simulation of old plant kinetic parameters, standard ore. Gamma unity

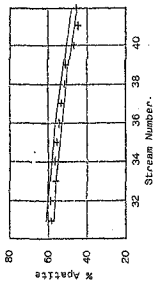
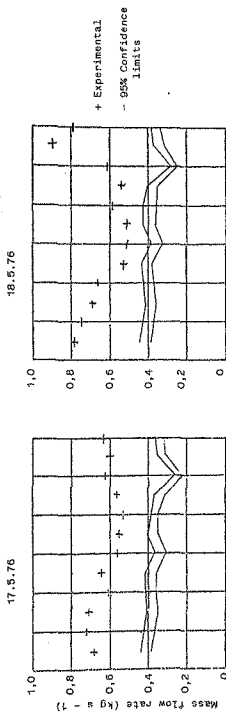


Figure 71 Simulation of old plant kinetic parameters, batch conditioned. Gamma unity

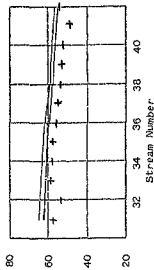


Figure 72 Simulation of old plant kinetic parameters, batch conditioned. Gamma unity

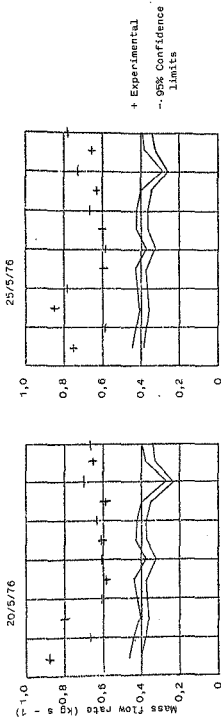


Figure 73 Simulation of old plant kinetic parameters, batch conditioned. Gamma unity.

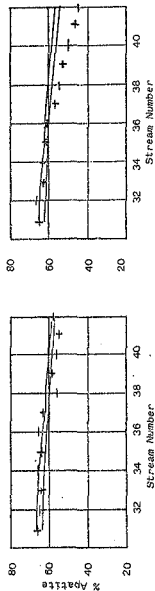


Figure 74 Simulation of old plant kinetic parameters, batch conditioned. Gamma unity.

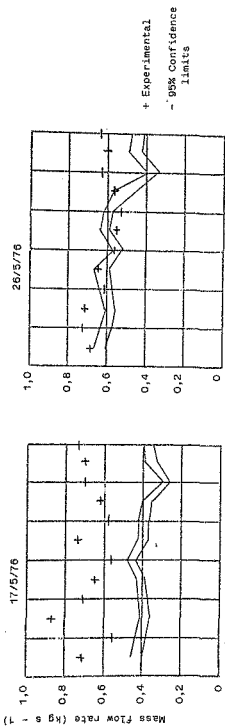


Figure 75 Simulation of old plant kinetic parameters, batch conditioned.  
Gamma unity

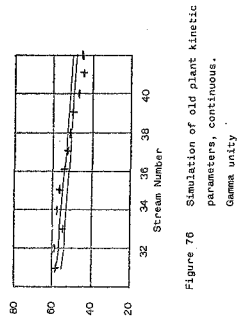


Figure 76 Simulation of old plant kinetic parameters, continuous.  
Gamma unity

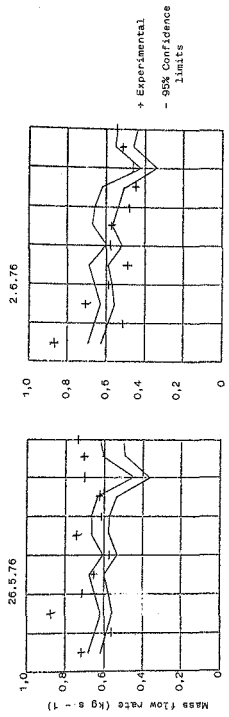


Figure 77 Simulation of old plant kinetic parameters, continuous. Gamma unity

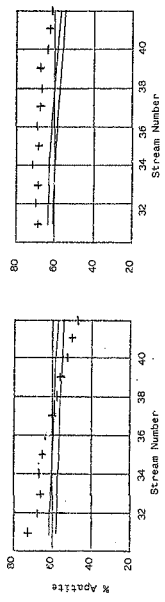


Figure 78 Simulation of old plant kinetic parameters, continuous. Gamma unity

+ Experimental  
- 95% Confidence limits

4.1.1 Simulations using gamma calculated from water ratio.

4.1.1.1 Percent apatite in concentrate streams

The model's prediction of the percent apatite in each concentrate stream is fairly closely modelled by the standard ore kinetic parameters, as shown by the experimental points falling within the 95% confidence interval generated by the model. Figs 51 - 56. In Figures 54 and 55 the final four and three experimental points respectively fall outside the 95% confidence band. The reason that the model does not allow a quick enough fall off in grade can be attributed to either the specific rate constant for apatite being too high or the specific rate constant for gangue too low.

The prediction of the apatite grade using the kinetic parameters from the conditioned rougher feed and continuous plant runs (Figs 57 - 64) all show the trend of over estimation of this variable, for the same reasons as stated above.

4.1.1.2 Mass flow rate in concentrate streams

In all cases, Figs 51 - 64, the estimation of the mass flow rate is too low, although the predicted curves do show the same trend as the experimental. The cause of this lack of fit can be attributed to one or a combination of the following factors, either there is not enough aeration in the cells, or the

specific rate constant for apatite is too low, or the froth transmission coefficient is too low.

4.1.2 Simulations using a gamma value of unity

4.1.2.1 Percent apatite in concentrate streams

The estimator gave good correlations between the predicted and experimental grade value in the concentrate streams when using the kinetic parameters of the standard ore series Fig 65 - 70, but once again there was significant lack of fit when using either the continuous or conditioned rougher feed kinetic parameters. Figs 71 - 78. The estimated curves show a shallower fall off than the observed, again indicating that either the specific rate constants for apatite are too high or those for gangue too low.

4.1.2.2 Mass flow rate in concentrate streams

The predictions using the standard ore and conditioned rougher feed kinetic parameters still show a lack of fit compared with the experimental, although the shape of the curve is followed showing that there is either too little aeration or the specific rate constant for apatite is low. Using the kinetic parameters from the continuous plant runs, the estimator gave a better fit to the experimental points, although some still fell outside the 95%

confidence region. It can be inferred from the better fit obtained using a higher specific rate constant for gangue and a froth transmission coefficient of one, that a closer fit might be obtained by increasing the aeration rate in the cells.

#### 4.2 Daily simulation of old plant

The simulator has two uses, the first is a detailed prediction of mass flows, grade and particle size distribution in each stream, which is of use when designing a flotation plant, and the other is a more gross use, where the simulator is only required to predict the final grade and recovery.

It has been shown that there is a lack of fit between the experimental and predicted curves in the detailed analysis of the old plant rougher bank, and that the fit could be improved by:-

- 1) increasing the specific rate constant for gangue
- 2) increasing the froth transmission coefficient to one
- 3) increasing the aeration rate.

Therefore using, as a starting point, the standard ore kinetic parameters, the above parameters were adjusted until a fit was obtained. The month of January was arbitrarily chosen for the adjustment of the kinetic parameters. They were altered until a "good" fit of predicted values to plant data was obtained. The parameters that were obtained in this way were then used to simulate the months of February through to June, i.e. parameters were adjusted once only. To establish the validity of these adjustments to the model parameters a daily simulation was carried out on the old plant for six months, and the experimental and predicted percent apatite and grade in the final concentrate were plotted. (Figs 79 - 84).

The data that was used for the daily simulations was as follows:-

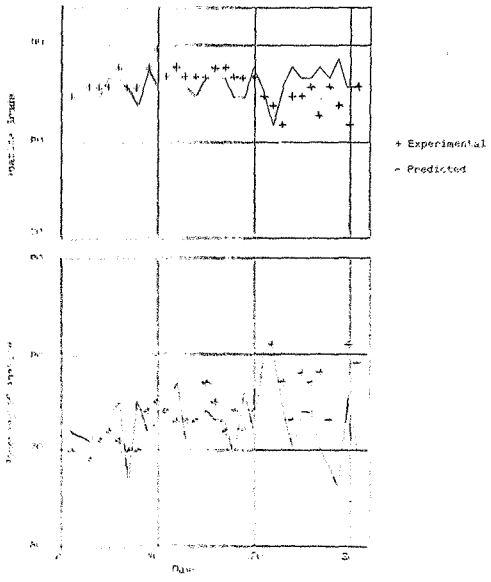


Fig. 20. Daily mean temperature and pressure, 1950-51, at the station. (1950-51, January 1951)

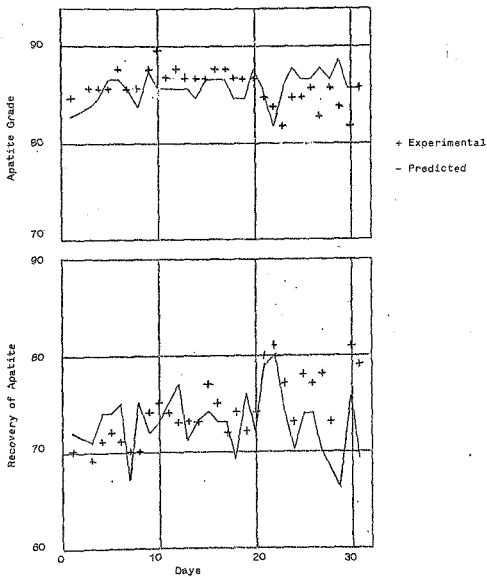


Table 79 Daily graph of experimental and predicted recovery and grade of apatite for January 1977

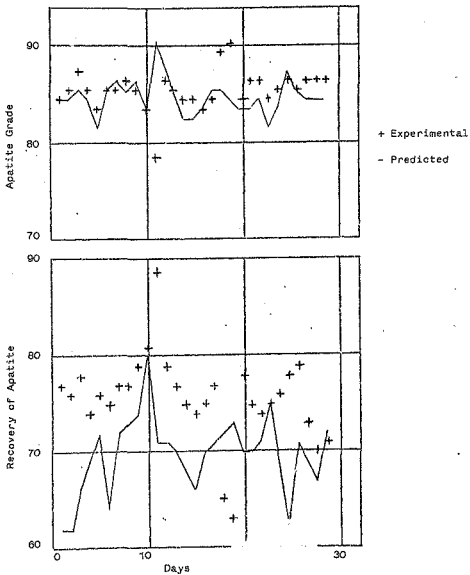


Table 80 Daily graph of experimental and predicted recovery and grade of apatite for February 1977

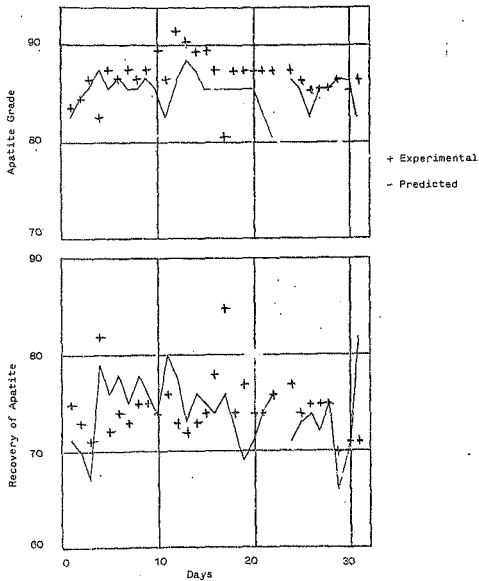


Table 81 Daily graph of experimental and predicted recovery and grade of apatite for March 1977

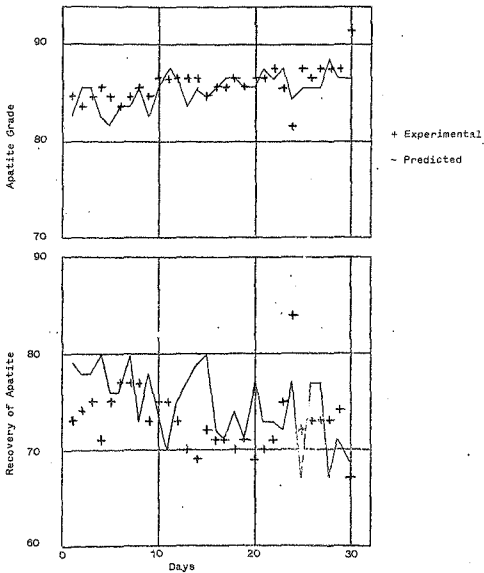


Table 82 Daily graph of experimental and predicted recovery and grade of apatite for April 1977

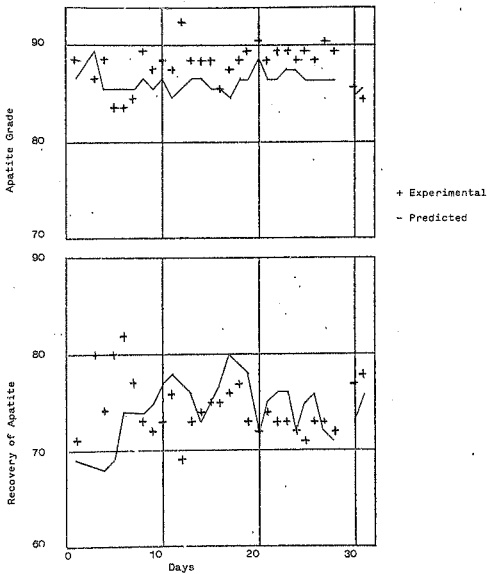


Table 83 Daily graph of experimental and predicted recovery and grade of apatite for May 1977

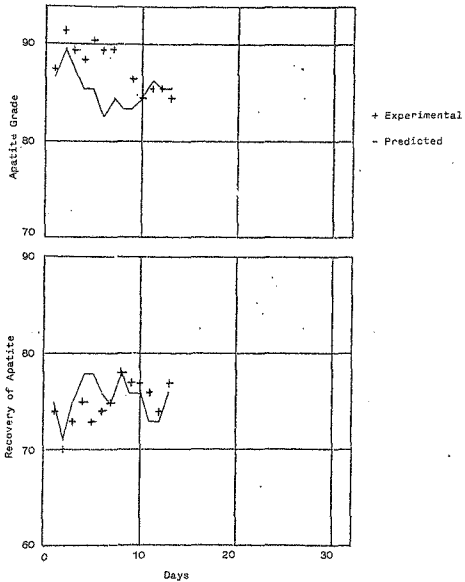


Table 84 Daily graph of experimental and predicted recovery and grade of apatite for June 1977

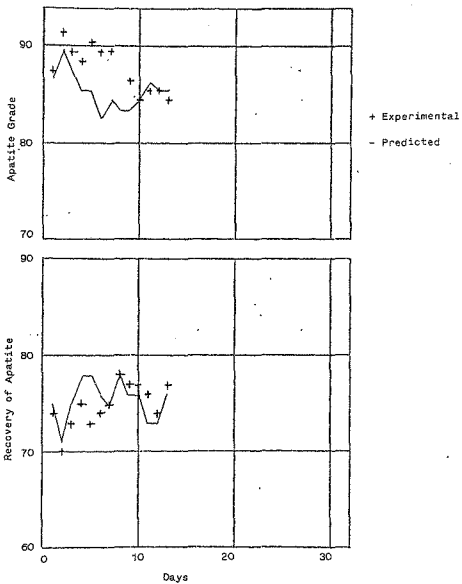


Table 84 Daily graph of experimental and predicted recovery and grade of apatite for June 1977

- 1) feed rate in metric tonnes per day
- 2) percent  $P_2O_5$  in feed
- 3) mass percent + 417 microns
- 4) mass percent - 208 microns

all of which were available from daily plant records.

It was found that a straight line fit was adequate in describing the relationship between mass percent and particle size, thus the simulator was adjusted so that the distribution of particles among D-classes could be calculated from the mass percent +417 micron and mass percent -208 micron size fractions. The distribution of particles among G-classes for each D-class was then back calculated using the daily percent  $P_2O_5$  value for the feed and the newly calculated distribution of particles among D-classes. It was assumed that the relative ratio between the particles in the G-classes for each D-class would remain constant.

The visual impression from Figs 79 - 84 tends to indicate that the apatite grade can be fairly accurately modelled, but the percent recovery of the apatite shows a lack of fit in some instances i.e. Fig 80., although the shape of the predicted curve follows the experimental. Upon a closer statistical investigation between the predicted and experimental data points the correlation coefficient for the apatite grade is 0.17 while that for the recovery of apatite is -0.01. This indicates that there is little correlation between the calculated and actual results for the apatite grade and virtually none between the recovery data points.

Notwithstanding this fact inferences can be drawn from these figures. It will be noticed that on days when there was a low feed rate (Fig 80, day 11 : Fig 81; days 4,17 : Fig 82; day 24) the predicted recovery is lower than the observed while the grade is higher. This would indicate that some other factor is operating on the system. The outside influence is the process operator. The operator's scenario is that apatite grade must be maintained at an average shift (8 hours) value of 34.6%  $P_2O_5$  (81.8% apatite). To achieve this grade value reagent combinations, addition rates and froth heights are varied. This operator factor may be interpreted as a type of froth transmission coefficient which is being continually adjusted, and no simulator, however, complex or sophisticated can allow for this type of interaction.

#### 4.3 Simulation of new plant

Having simulated the old plant using the kinetic parameters from the standard ore, conditioned rougher feed and continuous series, and finding that those parameters from the conditioned rougher feed gave the best fit, it was decided to scrutinize the suite of parameters obtained before embarking upon the simulation of the new plant. Unlike the simulation of the old plant, which consisted only of predicting the rougher bank, the simulation of the new plant also entailed the prediction of the performance of the scavenger, cleaner and recleaner.

A comparison of the kinetic parameters produced by King (17), on the same ore type, showed that there was a significant overlap in the 95% confidence regions of those kinetic parameters

estimated from the batch flotation of conditioned rougher feed and the 95% confidence regions of the average kinetic parameters of King's (Table 18). As one of the main purposes of this thesis was to determine whether or not it was possible to produce kinetic parameters in a batch cell that would predict what was happening on an industrial scale plant, it was decided to use the mean value of those parameters obtained from the conditioned rougher feed in predicting the new plant.

Data on four days (NP1, NP2, NP3, NP4) was collected from each cell in the new plant. This consisted of, mass percent solids, percent apatite per stage, water addition rates to the launders, assay sieve analysis of plant feed, final concentrate and tails, and also the fresh feed flow rate. It must be noted that the new plant consists of four banks of cells, as shown in figure , run in parallel. Thus the feed is split into four streams which go to conditioning tanks, where the reagents are added and then on to the banks of cells. The final tailings, stream 16, of each of the four banks are combined into a single stream which can then be sampled, similarly with the final concentrate streams (stream 52).

It was found that for each day, with small adjustments to one of the fractions floated and the froth transmission coefficient, that the final concentrate grade and recovery could be well simulated. The grades and recoveries were obtained from the daily log sheets at Foskor and are based on 24 hour composite samples analysed at the Foskor Analytical Laboratory. Table 19 shows the changes, on a day-to-day basis, of the fraction floated and froth transmission coefficient

estimated from the batch flotation of conditioned rougher feed and the 95% confidence regions of the average kinetic parameters of King's (Table 18). As one of the main purposes of this thesis was to determine whether or not it was possible to produce kinetic parameters in a batch cell that would predict what was happening on an industrial scale plant, it was decided to use the mean value of those parameters obtained from the conditioned rougher feed in predicting the new plant.

Data on four days (NP1, NP2, NP3, NP4) was collected from each cell in the new plant. This consisted of, mass percent solids, percent apatite per stage, water addition rates to the launders, assay sieve analysis of plant feed, final concentrate and tails, and also the fresh feed flow rate. It must be noted that the new plant consists of four banks of cells, as shown in figure 18, run in parallel. Thus the feed is split into four streams which go to conditioning tanks, where the reagents are added and then on to the banks of cells. The final tailings, stream 16, of each of the four banks are combined into a single stream which can then be sampled, similarly with the final concentrate streams (stream 52).

It was found that for each day, with small adjustments to one of the fractions floated and the froth transmission coefficient, that the final concentrate grade and recovery could be well simulated. The grades and recoveries were obtained from the daily log sheets at Foskor and are based on 24 hour composite samples analysed at the Foskor Analytical Laboratory. Table 19 shows the changes, on a day-to-day basis, of the fraction floated and froth transmission coefficient

Parameter	95% Confidence Regions	
	Average King	Average Conditioned Rougher Feed
FF13	0,782 - 0,932	0,874 - 1,0
FF22	0,877 - 1,0	0,747 - 1,0
KK 2	0,293 - 0,281	0,198 - 0,501
KK 3	0,736 - 1,20	1,056 - 1,293

Table 18 Comparison of 95% confidence regions

Parameters	Conditioned rougher feed	D A Y S			
		NP1	NP2	NP3	NP4
FF13	0,944	0,915	0,944	0,866	0,944
FF22	0,964	0,987	0,499	0,987	0,920
KK 2	0,357E+4	0,357E+4	0,357E+4	0,357E+4	0,357E+4
KK 3	0,118E+3	0,118E+3	0,118E+3	0,118E+3	0,118E+3
Gamma	-	0,892	0,783	0,648	0,765

Table 19 Comparison of kinetic parameters used to simulate new plant

with those obtained from the old plant conditioned rougher feed.

Table 20 gives the experimental and predicted percent  $P_2O_5$  and percent recovery from the final concentrate. As it can be seen from table 20, the fit between the experimental and predicted results are excellent, thus showing that the model is capable of not only predicting the grade but also the recovery of the final concentrate. More significant than this, is the fact, that the parameters which were used to predict the behaviour of the new plant, which consisted of 300 and 150 cubic foot cells, were obtained from a 3 litre batch flotation cell.

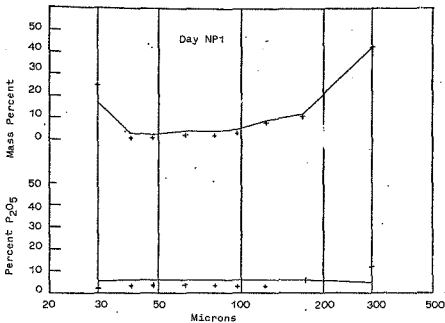
Thus in a global sense the simulator can be said to give good representation of the working plant. But the simulator to be of any true value must also be able to predict the finer details of the plant. An estimation of the power of the simulator can be obtained by an examination of the grade as a function of particle size and also the particle size distribution in the final concentrate and tails, as predicted by the simulator (Figures 85-88). In figures 85, 86 which show the grade and particle size distribution in the final tails, there is good agreement between experimental and predicted results.

The discrepancies in the largest and smallest particle size are probably due to the difficulty in determining the corresponding values in Colborn's  $Q(D)$  function. In figures 87, 88 which show the grade and particle size distribution in the final concentrate, there is good agreement between experimental and predicted results for the particle size distribution, except for the end values, which again can be attributed to the uncertainty of the corresponding values in the

Day	Percent P <sub>2</sub> O <sub>5</sub>		Percent Recovery	
	Experimental	Predicted	Experimental	Predicted
NP1	36,7	34,8	55,3	66,6
NP2	36,2	36,3	54,9	64,8
NP3	36,6	36,8	59,5	59,7
NP4	35,5	34,6	69,9	69,9

Table 20 Comparison between experimental and predicted grade and recovery of the final concentrate

FIGURE 85 ASSAY SIEVE ANALYSIS OF FINAL TAILS



+ Predicted  
- Experimental

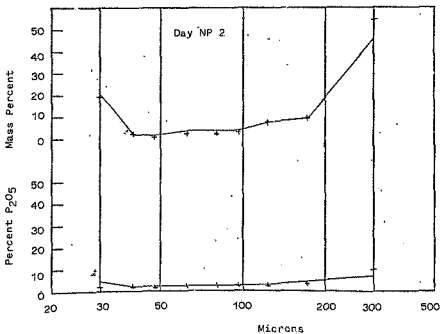


FIGURE 86 ASSAY SIEVE ANALYSIS OF FINAL TAILS

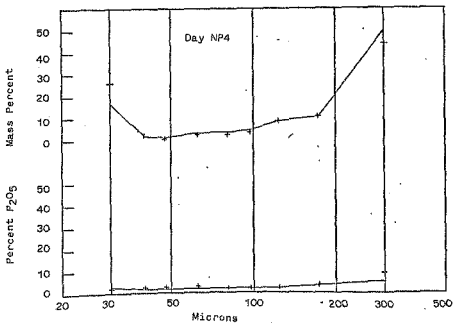
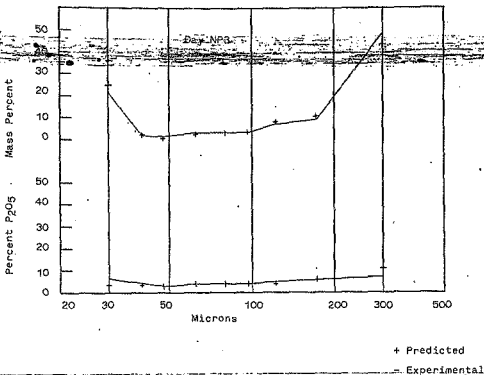


FIGURE 87 ASSAY SIEVE ANALYSIS OF FINAL CONCENTRATE

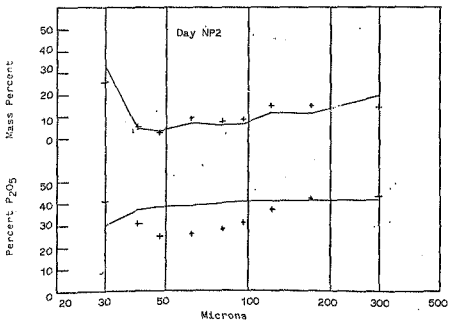
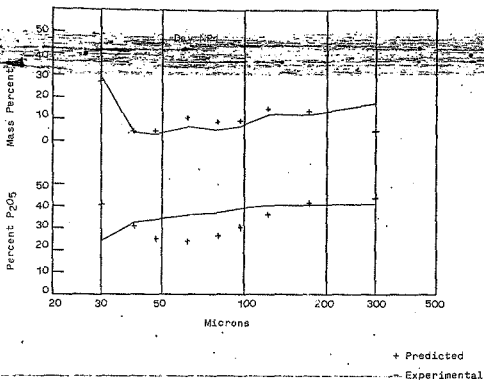
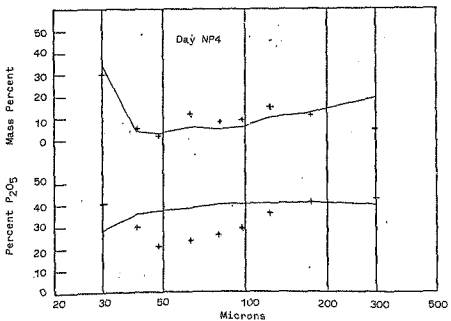
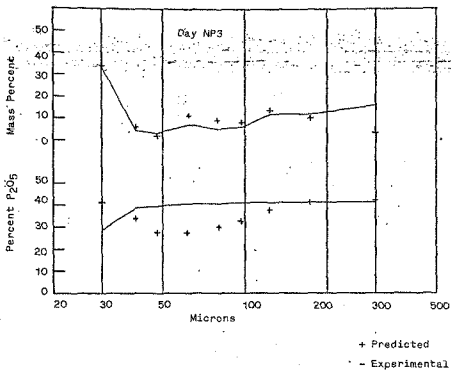


FIGURE 88 ASSAY SIEVE ANALYSIS OF FINAL CONCENTRATE



Colborn  $\Theta(D)$  function. It should be noted that the Colborn  $\Theta(D)$  function used was that obtained from the rougher feed in the old plant, and the simulator uses these values for the rougher, scavenger, cleaner and recleaner stages. The plot of grade as a function of particle size, on all four days, shows a lack of fit between experimental and predicted results. The reason for the dip in the predicted results can be attributed to the fact that too much gangue is reporting in the middle size ranges. A possible explanation for this is that the mean rate constant for the gangue is too high and/or Colborn's  $\Theta(D)$  function is incorrect, and this combined with the fact that the observed recirculating load was 100 percent of the fresh feed would probably cause a dip in the apatite grade.

It has been shown above, that the kinetic parameters give a final grade and recovery that agrees with the experimental results, and although it is not possible to predict the assay sieve analysis of the final concentrate and thus determine in which particle sizes the apatite reports, an examination of the grade along the new plant bank would give an estimate of the significance of the kinetic parameters. Figures 89, 92 show the experimental and predicted percent  $P_{205}$  for each stage of the new plant.

From these figures it can be seen that the simulator gives a good description of the cleaner and recleaner (streams 41 - 48) on all four days, also of the rougher and scavenger on day NP2. For the other three days the simulator shows a too steep fall off in the rougher and scavenger. It is significant to note that even when the simulator fails to predict the rougher and scavenger it is still able to predict the cleaner and recleaner. To explain the lack of fit in the rougher and scavenger the following are postulated:-

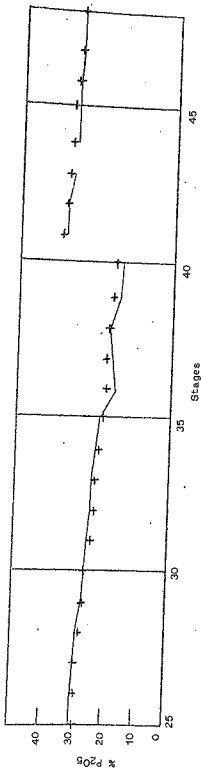


Figure 90 Percent P<sub>2</sub>O<sub>5</sub> per stage for day NP2

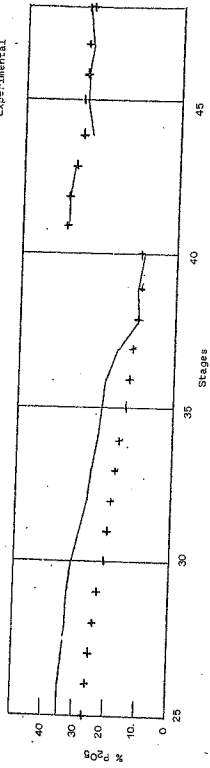


Figure 89 Percent P<sub>2</sub>O<sub>5</sub> per stage for day NP1

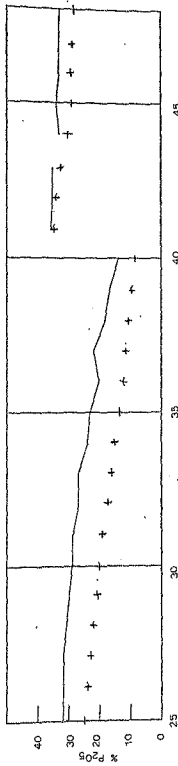


Figure 92 Percent P<sub>2</sub>O<sub>5</sub> per stage for day NP4

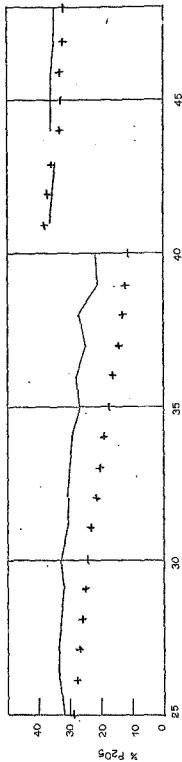


Figure 91 Percent P<sub>2</sub>O<sub>5</sub> per stage for day NP3

1. The froth transmission coefficient is incorrect.
2. Due to the large recirculating load (100%), a small error in the mean values of the kinetic parameters associated with the gangue could cause too much gangue to be recovered and thus recycled.
3. The simulations have been restricted to the simple case where each mineral has been regarded as only having a floatable and a non-floatable component, with nothing in between.

CHAPTER 5.

DISCUSSION AND CONCLUSIONS

5.1 Kinetic Parameters

It has been demonstrated that within experimental limits, that there is no unique value for any of the kinetic parameters. Further, by using the same ore type, but varying the conditioning, different values of the kinetic parameters are obtained. The reasons for this lack of coherent results may be enumerated thus:-

- 1) conditioning time
- 2) reagent combination
- 3) reagent addition rates.

The batch tests carried out on the unconditioned feeds, indicate that the above three variables can be minimized, as shown by the estimated kinetic parameters having very similar values.

The conditioning time has the greatest effect upon the reproductibility of experimental results as shown by the narrow 95% confidence limits of the kinetic parameters for the batch tests on the conditioned rougher feed. It is possible to explain the effect of prolonged conditioning upon the kinetic parameters in terms of the reagent contact time, i.e., the longer the contact time the more reagent will adsorb on to the mineral species. To test this hypothesis out on the batch flotation of unconditioned feed would be difficult due to the variability of the experimental results. It would be more beneficial to determine the adsorption isotherms of the various minerals with respect to each of the reagents. From these isotherms the optimum conditioning time for the ore could be

determined and float tests carried out to verify the results. The optimum conditioning time should minimize the experimental variation in the kinetic parameter estimates.

### 5.2 Froth Transmission Coefficient

Of all the primary data required to calculate the kinetic parameters, and also run the simulation model, the froth transmission coefficient is the least amenable to measurement. It has been shown, in the simulation of the old plant rougher bank that its value lies between the one calculated from the water ratio and unity.

To obtain a true value of the froth transmission coefficient, the froth must be sampled as it is formed, i.e., at the pulp/froth interface. The designing of an interface sampling apparatus presents few difficulties if its use is confined to the laboratory or pilot plant scale work where the pulp density, aeration rate, impeller speed and froth height are carefully controlled. In an operating plant the aeration is such that it causes turbulence over the whole surface area of the cell, thus the pulp/froth interface is unstable and non-uniform. Therefore until such time as apparatus can be designed to cope with a normal operating plant, the value of the froth transmission coefficient can only be estimated from the water ratio in the concentrate streams.

### 5.3 General

Previous workers using Foskorite ore have shown

that the simulator is capable of predicting a single batch cell and a continuous running pilot plant. The lack of fit of the simulator for a "real" continuous operating plant can be explained as follows. The system upon which the previous work was carried out, was one in which the variables were closely monitored, but more important than this the ore type remained constant. Thus in all cases the test work was carried out on the same batch of ore. The kinetic parameters, whether obtained via batch or continuous test work would be expected to be the same or very close. Under these "ideal" conditions plant configurations can be tested against theory, but in practical terms the simulator can only give an indication of the best possible plant configuration to maximize the grade and recovery.

It has been amply demonstrated throughout this work that the simulator in its present state is incapable of being used for daily predictions of plant grade or recovery, and that the detailed analysis for each stage cannot be adequately simulated, thus no indication of the best plant configuration can be obtained.

REFERENCES.

1. Loveday, B.K., Analysis of froth flotation kinetics. Trans. Instn. Min. Metall., 75, C219 (1966)
2. Woodburn, E.T. and Loveday, B.K. The effect of variable residence time on the performance of a flotation system. J.S. Afr. Inst. Min. Metall., 65, 612 (1965)
3. Preller, G.S., Ph.D thesis Potchefstroom University 1965
4. Hanekom, H.J., et al. The Geology of the Phalaborwa Igneous Complex. Dept. of Mines Geological Survey Memoir 54
5. Taggart, A.F., Handbook of mineral dressing 22.67
6. Mika, Y.S., and Fuerstenau, D.W., A microscopic model of the flotation process. Mezhdwaradnyi Kongres po Oboyashenuja Poleznyka Isokolaenyya II Izdanie Instituta, Mekhanobv Leningrad pp 246 - 269 (1969)
7. Pogorely, A.D., Limits of the use of the kinetic equation proposed by K.F. Seloglazov, Izv. Vuz. Tsvetnaya Metallurgia, No. 1, pp 33 - 40 (1962)
8. Engelbrecht, J.A., Full scale flotation plant data for modelling purposes. NIM report 1753 (1975)
9. Woodburn, E.T., King, R.P., and Colborn, R.P. The effect of particle size distribution on the performance of a phosphate flotation process. Met Trans vol 2 p 2136 (1971)
10. King, R.P., and Moys, M.H., A computer program for the estimation of parameters in flotation. NIM report 1558 (1973)
11. Loveday, B.K., Analysis of froth flotation kinetics. Trans Instn. Min. Metall., 75, C219 (1966)

12. Moys, M.H., et al. Estimation of parameters in the distributed-constant flotation model. NIM report 1567 (1973)
13. Davey, W. An experimental investigation of the conditioning of an apatite ore for flotation. MSc thesis, University of Natal 1973
14. King, R.P., Flotation research work of the N.I.M. Research group, and the Department of Chemical Engineering, University of Natal. J. S.A. Inst. Min. and Met. 135 (1972)
15. King, R.P., A computer program for the simulation of the performance of a flotation plant NIM report 1435 (1973)
16. De Waal, F. Fosker report. An examination of the capacity of Sala Pumps for F section middlings (15.11.76)
17. King, R.P. A pilot-plant investigation of a kinetic model for flotation NIM report 1847 (1976)
18. King, R.P., A pilot-plant investigation of a kinetic model for flotation. To appear in J. SAIMM. (1976)
19. Analytical Chemistry Vol 46 No. 11 Sept 1974 p 1614 - 1615
20. Hayslett H.T. Statistics Made Simple p 152 - 156 (1967)

APPENDIX 1

MEASUREMENT OF SPECIFIC GRAVITY.

The method employed utilizes the fact that calibrated micro-syringes are able to deliver small volumes of liquids with extremely high precision and accuracy. Such syringes are rated to deliver an accuracy of  $\pm 1\%$  of the volume delivered.

PROCEDURE

A sample of liquid was drawn into the syringe. All bubbles were removed by inverting the syringe and tapping it gently. The plunger was set at the volume mark 0,3, and the tip of the needle was cleaned with a paper tissue. The mass of the syringe plus contents was then determined and recorded. The sample was expelled from the syringe, the tip was again cleaned, and the syringe re-weighed. The density was calculated from the difference in the two weights divided by the corrected volume charge taken. (19)

The syringe was calibrated using distilled water at a known temperature, thus the corrected volume of the syringe was obtained.

APPENDIX 2      Replicate analysis by Foskor's Analytical  
Laboratory

Experiment number	Percent P <sub>2</sub> O <sub>5</sub>	Percent P <sub>2</sub> O <sub>5</sub>
	1st assay	2nd assay
P48/T	2,9	2,8
P48/S	29,6	29,7
P51/T	2,7	2,7
P49/2	22,5	22,6
P51/2	19,4	19,7
P48/6	16,1	16,8
P52/5	12,0	11,9
P50/6	10,6	10,9
P51/3	12,9	13,1
P52/3	13,3	13,5
P52/2	18,8	18,9
P50/2	22,9	23,0
P50/5	28,4	28,0
P50/7	11,2	11,3
P52/4	14,5	14,6
P49/T	2,8	2,9
P48/T	2,8	2,8
P49/B	11,4	11,3
P53/T	2,4	2,3
P53/S	27,0	26,9

Experiment number	Percent P <sub>2</sub> O <sub>5</sub> 1st assay	Percent P <sub>2</sub> O <sub>5</sub> 2nd assay
RF/35	16,6	16,5
RF/42	23,8	24,4
RF/52	25,1	24,9
RF/33	22,1	22,3
RF/51	24,0	24,7
RF/31	24,5	24,5
RF/44	20,1	19,9
P50/T	2,0	1,8
P49/5	24,7	24,9
P49/5	12,3	12,7
Total	496,3	499,3
Average % Error	0,60	

Table 2.1 Replicate results, and their average percent error

APPENDIX 3

HEAVY LIQUID SEPARATION

In the following tables the results of the heavy liquid separation on the magnetic and non-magnetic samples as separated from the Frantz Isodynamic Separator are given

Transverse angle + 0	
Density	Cumulative float fraction
2,69	0,028
2,72	0,092
2,73	0,213
2,74	0,406
2,77	0,525
2,90	0,546
3,08	0,554
3,15	0,581
3,16	0,640
3,19	0,824
3,22	0,987

Table 3.1 Density vs. cumulative float fraction of material collected at transverse angle +0

Transverse angle + 2	
Density	Cumulative float fraction
2,73	0,168
2,75	0,489
2,81	0,641
2,95	0,663
3,08	0,676
3,15	0,716
3,16	0,776
3,22	0,990

Table 3.2 Density vs. cumulative float fraction of material collected at transverse angle +2

Transverse angle + 4	
Density	Cumulative float fraction
2,70	0,058
2,71	0,183
2,78	0,511
2,83	0,566
2,95	0,623
3,08	0,642
3,15	0,688
3,16	0,760
3,22	0,985

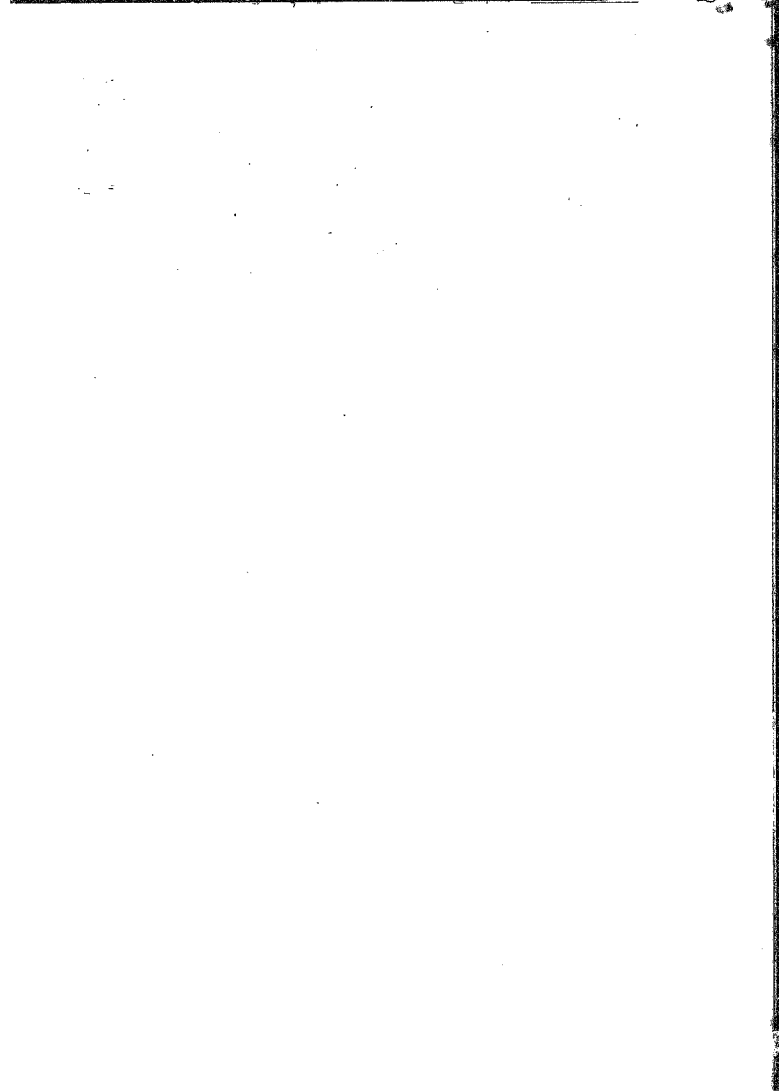
Table 3.3 Density vs. cumulative float fraction of material collected at transverse angle +4

Transverse angle + 6	
Density	Cumulative float fraction
2,74	0,171
2,80	0,456
2,83	0,482
2,87	0,523
2,88	0,558
2,95	0,587
3,08	0,610
3,15	0,656
3,16	0,729
3,22	0,985

Table 3.4 . Density vs. cumulative float fraction of material collected at transverse angle +6

Transverse angle - 0 (non-magnetic fraction)	
Density	Cumulative float fraction
2,75	0,092
2,81	0,111
2,90	0,113
2,95	0,120
3,08	0,123
3,14	0,145
3,18	0,221
3,22	0,958

Table 3.5 Density vs. cumulative float fraction of material collected at transverse angle -0



**Author** Burton Phillip Frederick

**Name of thesis** A Simulation Of The Foskor Flotation Plant. 1978

***PUBLISHER:***

University of the Witwatersrand, Johannesburg

©2013

***LEGAL NOTICES:***

**Copyright Notice:** All materials on the University of the Witwatersrand, Johannesburg Library website are protected by South African copyright law and may not be distributed, transmitted, displayed, or otherwise published in any format, without the prior written permission of the copyright owner.

**Disclaimer and Terms of Use:** Provided that you maintain all copyright and other notices contained therein, you may download material (one machine readable copy and one print copy per page) for your personal and/or educational non-commercial use only.

The University of the Witwatersrand, Johannesburg, is not responsible for any errors or omissions and excludes any and all liability for any errors in or omissions from the information on the Library website.